JGR Oceans

RESEARCH ARTICLE
10.1029/2024JC021862

Nitrate-Nitrite Isotopic Exchange: Unveiling Its Influence on Isotope Effect Estimates in Nitrate Assimilation in the Cosmonaut Sea, Antarctica

Xueli Ba[1], Jun Zhao[2], Minfang Zheng[1], Mengya Chen[1], Jiawen Kang[1], Jiashun Hu[1], Shunan Cao[3], Jianfeng He[3], and Min Chen[1]

[1]College of Ocean and Earth Sciences, Xiamen University, Xiamen, China, [2]Second Institute of Oceanography, Ministry of Natural Resource, Hangzhou, China, [3]Polar Research Institute of China, Shanghai, China

Key Points:

- Isotope systematics reveal isotopic exchange between nitrate and nitrite, highlighting the complexity of nitrogen cycle
- Isotopic exchange between nitrate and nitrite influences the estimates of isotope effects in nitrate assimilation
- Reduced nitrate assimilation isotope effects observed south of the SB may be associated with iron-rich conditions

Correspondence to:
M. Chen,
mchen@xmu.edu.cn

Citation:
Ba, X., Zhao, J., Zheng, M., Chen, M., Kang, J., Hu, J., et al. (2025). Nitrate-nitrite isotopic exchange: Unveiling its influence on isotope effect estimates in nitrate assimilation in the Cosmonaut Sea, Antarctica. *Journal of Geophysical Research: Oceans*, *130*, e2024JC021862. https://doi.org/10.1029/2024JC021862

Received 17 SEP 2024
Accepted 5 MAY 2025

Author Contributions:
Conceptualization: Xueli Ba, Min Chen
Data curation: Minfang Zheng, Mengya Chen
Formal analysis: Xueli Ba, Jun Zhao, Jiawen Kang
Funding acquisition: Min Chen
Investigation: Jiawen Kang, Jiashun Hu
Methodology: Xueli Ba, Jun Zhao
Project administration: Jianfeng He
Resources: Minfang Zheng, Mengya Chen, Shunan Cao
Supervision: Min Chen
Validation: Jun Zhao, Minfang Zheng
Visualization: Xueli Ba
Writing – original draft: Xueli Ba
Writing – review & editing: Shunan Cao, Jianfeng He, Min Chen

Abstract Recent insights into isotopic exchange between nitrate and nitrite have introduced complexities to our understanding of the nitrogen cycle in the Southern Ocean. This study highlights unusual isotopic compositions in the mixed layer of the Cosmonaut Sea characterized by notably low $\delta^{15}N$ and high $\delta^{18}O$ values in nitrite. These anomalies challenge our expectations regarding isotopic behavior within cycling pathways, highlighting the significant role of isotopic exchange between nitrate and nitrite. Interestingly, incorporating this exchange reaction significantly altered the estimated isotope effect of nitrate assimilation for both nitrogen and oxygen based on the Rayleigh model in the nitrate-only system. This raises questions about the reliability of previous estimates in assessing nitrate consumption in the Southern Ocean, suggesting that the nitrate + nitrite system may provide a more accurate representative of nitrate uptake. Additionally, spatial variations in the nitrate assimilation isotope effect ($\varepsilon_{NO_3+NO_2}$) both for nitrogen and oxygen were also observed, with higher $^{15}\varepsilon_{NO_3+NO_2}$ and $^{18}\varepsilon_{NO_3+NO_2}$ values north of the southern boundary (SB) and lower values to the south. The reduced $^{15}\varepsilon_{NO_3+NO_2}$ and $^{18}\varepsilon_{NO_3+NO_2}$ values south of the SB may be primarily driven by elevated iron concentrations as indicated by the positive relationship between $^{18}\varepsilon_{NO_3+NO_2}$ and $\triangle Si/\triangle N$, a proxy for iron limitation, rather than by nitrification, phytoplankton composition, vertical mixing, or light availability. This study uses dual isotopes of nitrate and nitrite to evaluate isotopic exchange effects on nitrate assimilation, specifically for oxygen, enhancing our understanding of the Southern Ocean's role in the global nitrogen cycle.

Plain Language Summary Nutrient consumption in the Southern Ocean is pivotal for global nutrient cycles. The isotope fractionation of nitrate assimilation serves as an effective indicator of nitrate utilization and is extensively applied in paleoceanographic reconstructions. However, recent studies have identified isotopic exchange between nitrate and nitrite, complicating traditional methodologies. It remains uncertain whether this exchange reaction impacts the fractionation factor derived solely from nitrate isotopes. This study, conducted in the Cosmonaut Sea in Antarctica, demonstrates that nitrate-nitrite isotopic exchange leads to unusually low $\delta^{15}N$ values and elevated $\delta^{18}O$ values in nitrite. This exchange not only alters the nitrogen and oxygen isotopic composition of nitrate but also influences the estimated isotope effect of nitrate assimilation based on the Rayleigh model both for nitrogen and oxygen. Furthermore, the isotope effect exhibits spatial variability with significantly lower values observed south of the Southern Boundary of the Antarctic Circumpolar Current, primarily attributed to increased iron availability, as inferred from the positive relationship between $^{18}\varepsilon_{NO_3+NO_2}$ and $\triangle Si/\triangle N$, a proxy for iron limitation. Consequently, lower isotope effect values should be utilized when reconstructing historical changes in nitrate consumption in Antarctic coastal waters.

1. Introduction

The Southern Ocean has significant potential to absorb carbon dioxide (CO_2) from the atmosphere, thereby playing a crucial role in regulating global climate change (DeVries, 2014; Gruber et al., 2023). Variations in the productivity of the Southern Ocean are considered primary drivers of atmospheric CO_2 fluctuations during glacial and interglacial periods, which, in turn, influence atmospheric temperature changes (Gray et al., 2018; Sarmiento & Toggweiler, 1984; Siegenthaler & Wenk, 1984; Sigman et al., 2010). Additionally, nutrients supplied by the upwelling of Circumpolar Deep Water (CDW) in the Southern Ocean are partially transported horizontally to the thermocline of mid- and low-latitudes via mode water and intermediate water. These nutrients subsequently mix into the euphotic zone, impacting nutrient input and the biological pump in mid- and low-latitude oceans. Consequently, the Southern Ocean acts as a crucial gateway for regulating the global nutrient cycle and the

functioning of the biological pump (DeVries, 2014; Gruber et al., 2023; Nissen et al., 2021; Sarmiento et al., 2004). Major nutrients in the Southern Ocean, such as dissolved inorganic nitrogen (DIN) and dissolved inorganic phosphorus (DIP), are not fully depleted throughout the year due to limitations imposed by factors such as light and trace nutrients such as iron. However, their consumption reflects the fluctuating state of primary productivity in the Southern Ocean (Mitchell et al., 1991; Tagliabue et al., 2014).

Phytoplankton preferentially assimilate ^{14}N and ^{16}O during nitrate assimilation, leading to an enrichment of ^{15}N and ^{18}O in the remaining nitrate (Fripiat et al., 2019; Sigman et al., 1999). As phytoplankton consume nitrate, the $\delta^{15}N$ in nitrate ($\delta^{15}N_{NO3} = {}^{15}N/{}^{14}N)_{sample}/{}^{15}N/{}^{14}N)_{air} - 1$) gradually increases. Under a constant isotopic fractionation effect (ε), the $\delta^{15}N$ in newly formed suspended and settling particulate nitrogen ($\delta^{15}N_{PN}$) will increase accordingly (Altabet & Francois, 1994; Mariotti et al., 1981). The isotope effect of nitrate assimilation is defined as ${}^{15}\varepsilon = \left({}^{14}k/{}^{15}k - 1\right) \times 1000‰$, and ${}^{18}\varepsilon = \left({}^{16}k/{}^{18}k - 1\right) \times 1000‰$, where k is the kinetic reaction rate constant for each isotope (Casciotti, 2016b; Karsh et al., 2003). Both $\delta^{15}N_{PN}$ and $\delta^{15}N_{NO3}$ are used to estimate isotope effects during nitrate assimilation. However, the processes influencing $\delta^{15}N_{PN}$ are more complex, including PN degradation and ammonium uptake (Casciotti, 2016a). Therefore, $\delta^{15}N_{NO3}$ is a better choice for estimating the isotope effects of nitrate assimilation by phytoplankton. When estimating the fraction of nitrate drawn down using $\delta^{15}N_{NO3}$, two important parameters must be determined: the $\delta^{15}N_{NO3}$ signature of the nitrate source and the isotope effect of nitrate assimilation (Altabet & Francois, 1994). In the Southern Ocean during winter, sea ice formation and strong wind-induced mixing often create a deep mixed layer. In summer, increased solar radiation promotes sea ice melting, resulting in a shallower mixed layer than in winter, and forming a T_{min} layer with the lowest temperature beneath the warmer mixed layer. T_{min} retains the characteristics of winter water and serves as the initial source of nitrate for phytoplankton in the summer mixed layer (Altabet & Francois, 2001; DiFiore et al., 2010; Kemeny et al., 2016). The strong seasonality in the uptake to supply ratio allows the Rayleigh model to be a reliable approximation for isotopic fractionation during nitrate assimilation in the Antarctic Zone. Despite vertical supply in the summer, the comparatively high uptake rates allow the system to be considered closed (DiFiore et al., 2009; Fripiat et al., 2019; Kemeny et al., 2016). In the Rayleigh model of nitrate uptake by phytoplankton, the $\delta^{15}N_{NO3}$ and $\delta^{18}O_{NO3}$ in the surface mixed layer will have a linear relationship with $\ln[NO_3]$, with the slopes representing the nitrogen isotope effect (${}^{15}\varepsilon$) and oxygen isotope effect (${}^{18}\varepsilon$), respectively, and the intercepts representing the isotopic composition of the initial nitrate (DiFiore et al., 2006, 2009; Fripiat et al., 2019; Mariotti et al., 1981). Laboratory culture experiments have shown that $\delta^{18}O_{NO3}$ and $\delta^{15}N_{NO3}$ vary in a 1: 1 ratio, indicating that the ${}^{18}\varepsilon$ and ${}^{15}\varepsilon$ of nitrate assimilation by phytoplankton are similar (Granger et al., 2004, 2010).

Previous studies have investigated the isotope effects of nitrate assimilation in the Southern Ocean, examining the spatial and temporal variations of ${}^{15}\varepsilon$ and ${}^{18}\varepsilon$ (Altabet & Francois, 2001; DiFiore et al., 2009; Sigman et al., 1999; Smart et al., 2015). Winter ${}^{15}\varepsilon$ has been observed to range from 1.6 to 3.3‰, which is lower than summer values partially due to a lower uptake to supply ratio that introduces low-$\delta^{15}N$ nitrate into the winter mixed layer (DiFiore et al., 2010; Sigman et al., 1999; Smart et al., 2015). In summer, ${}^{15}\varepsilon$ shows a decreasing trend toward the poles accompanied by an increase in mixed layer depth (MLD), suggesting that light may significantly influence the isotope effect of nitrate assimilation (DiFiore et al., 2010; Needoba & Harrison, 2004). However, the poleward trends reported by DiFiore et al. (2010) may be influenced by differences in estimates derived from acidified versus nonacidified samples (Fripiat et al., 2019). The ${}^{15}\varepsilon$ in the Subantarctic Zone exceeds 7‰ (DiFiore et al., 2006) and is approximately 5‰ in the Antarctic Zone (DiFiore et al., 2009; Jang et al., 2008; Sigman et al., 1999). Recent findings indicate that the ${}^{15}\varepsilon$ values on the continental shelf of the West Antarctic Peninsula are between 2 and 6‰, with most sites significantly lower than 5‰, attributed to the influence of nitrification (Henley et al., 2017, 2018). The significant spatiotemporal variability underscores the importance of accurately estimating isotope effects in different Antarctic regions, as varying isotope effects may be necessary to determine the extent of nitrate consumption in different areas.

The isotope effect of nitrate assimilation is influenced by light conditions, iron availability, and phytoplankton composition. The ε is higher under lower light conditions (Needoba & Harrison, 2004) and lower under iron-enriched conditions (Karsh et al., 2003). Laboratory experiments have shown that the nitrogen isotope effect during nitrate assimilation varies with phytoplankton composition with eukaryotes exhibiting values from 5 to 8‰, whereas cyanobacterial strains do not exceed 5‰ (Granger et al., 2004, 2010). Studies on the enzyme mechanisms of nitrate assimilation reveal that isotopic fractionation primarily occurs during the intracellular

reduction of nitrate to nitrite, with intracellular enzymes affecting both $^{15}\varepsilon$ and $^{18}\varepsilon$ almost equally, around 26.6‰ (Karsh et al., 2012). The degree of isotopic fractionation in nitrate assimilation can be expressed as $\varepsilon_{org} = \varepsilon_{in} + f \cdot (\varepsilon_{nr} - \varepsilon_{out})$, where f represents the ratio of efflux to uptake. Under low light conditions, the rate of nitrate absorption by phytoplankton exceeds the rate of assimilation, leading to higher efflux of nitrate with elevated $\delta^{15}N$ values from the cells (Needoba & Harrison, 2004). Higher iron concentrations in the environment may enhance the intracellular reduction of nitrate and decrease the efflux of extracellular nitrate, resulting in lower ε (Karsh et al., 2003, 2012; Li et al., 2023; Smith et al., 2021; Takeda, 1998).

Recent studies have identified an isotope exchange process between nitrate and nitrite in the Southern Ocean, mediated by nitrite-oxidizing bacteria (NOB) through the nitrite oxidoreductase enzyme (NXR) (Chen et al., 2022, 2023; Fripiat et al., 2019; Kemeny et al., 2016). The NXR enzyme in NOB catalyzes both the oxidation of nitrite to nitrate and the reduction of nitrate to nitrite (Daims et al., 2016; Kemeny et al., 2016; Koch et al., 2015; Sundermeyer-Klinger et al., 1984). During this process, nitrate becomes enriched in ^{15}N, whereas nitrite is enriched in ^{14}N without altering $\delta^{15}N_{NO_3+NO_2}$ (Buchwald & Casciotti, 2010; Casciotti, 2009). The impact of isotope exchange between nitrate and nitrite on oxygen is more complex due to the abiotic exchange between nitrite and water (Casciotti et al., 2007). Laboratory incubation experiments labeled with ^{18}O demonstrate that both nitrate and nitrite exhibit oxygen isotope exchange with water, and the presence of nitrite-oxidizing microorganisms promotes the incorporation of oxygen atoms from water into nitrate (Friedman et al., 1986; Wunderlich et al., 2013). Kemeny et al. (2016) and Fripiat et al. (2019) observed no significant difference between measured nitrate-only $\delta^{18}O$ and nitrate + nitrite $\delta^{18}O$. Additionally, the $^{18}\varepsilon$ values derived solely from NO_3^- profiles show no significant difference compared to those derived from NO_3^- + NO_2^- profiles. Chen et al. (2022, 2023) later discovered extremely high $\delta^{18}O$ values of nitrite in the Southern Ocean, attributing this to oxygen isotope exchange between nitrite and nitrate. Assuming isotopic equilibrium between nitrate and nitrite, they estimated the NXR-mediated oxygen isotope equilibrium effect of the exchange reaction as 37.6 ± 3.5‰ based on their isotopic differences. The NXR-mediated nitrogen isotope equilibrium of the isotope exchange reaction between nitrate and nitrite is estimated to range from −69.2‰ to −55‰ based on molecular vibrational frequencies (Casciotti, 2009; Kemeny et al., 2016) and is estimated to be −53.9 ± 6.4‰ based on the measured nitrogen isotopic composition of nitrite (Chen et al., 2022). Considering that the concentration of nitrite in the Southern Ocean is only about 1% of that of nitrate, this substantial isotope effect will significantly alter the $\delta^{15}N$ of nitrite. Fripiat et al. (2019) determined the isotopic composition of nitrate and the combined nitrate + nitrite, finding that $\delta^{15}N_{NO_3}$ was approximately 0.7‰ higher compared to $\delta^{15}N_{NO_3+NO_2}$. They also demonstrated that the nitrogen isotope effect associated with nitrate assimilation derived solely from nitrate was significantly greater than that based on the combined nitrate + nitrite. Furthermore, the nitrogen isotope effect based on the combined nitrate + nitrite was relatively stable (5.5 ± 0.6‰) consistent with the $\delta^{15}N$ measurements of sediment trap particles. These findings suggest that nitrate + nitrite represents the assimilated pool on a seasonal basis as equilibrium exchange between nitrate and nitrite occurs within a closed system (Fripiat et al., 2019; Kemeny et al., 2016). Consequently, the isotope effect derived from nitrate + nitrite is likely a more reliable indicator of nitrate consumption. However, it remains uncertain whether such exchange influences the $\delta^{18}O$ value of nitrate and the estimated oxygen isotope effect of nitrate assimilation, as a comprehensive assessment is hindered by limited $\delta^{18}O$ measurements of nitrite.

In this study, we measured the nitrogen and oxygen isotopic composition of nitrate and nitrite in the Cosmonaut Sea, East Antarctica. By comparing the nitrogen and oxygen isotope effects of nitrate assimilation estimated through different methods, we clarified whether isotope exchange between nitrate and nitrite influenced the estimated isotope effect of nitrate assimilation. Additionally, we explored the spatial variation in the isotope effects of nitrate assimilation across the high-latitude regions of the Southern Ocean, with a particular focus on changes in coastal waters, and discussed potential reasons for this spatial variation.

2. Methods

2.1. Regional Setting

The Cosmonaut Sea is located west of Enderby Land and north of Ann Cape within the Indian sector of the Southern Ocean between 30 and 60°E (Hunt et al., 2007). The surface circulation in this area is primarily influenced by the eastward-flowing Antarctic Circumpolar Current (ACC), the westward-flowing Antarctic Coastal Current, and the clockwise Weddell Gyre, which affects the western part of the region (Williams

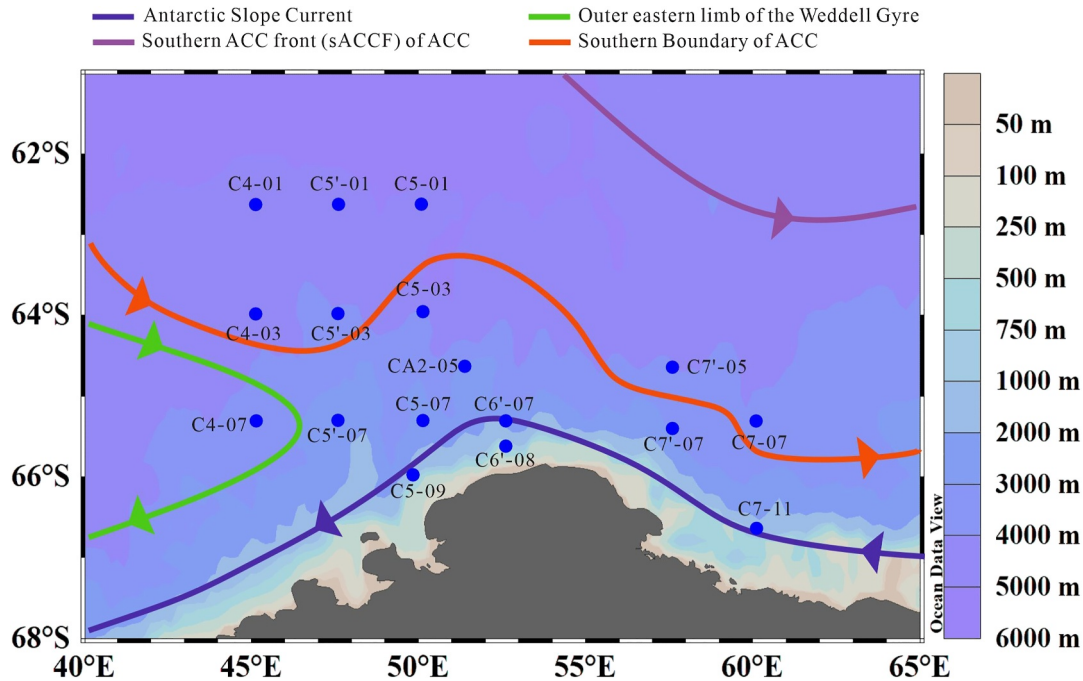

Figure 1. Map of sampling locations in the Cosmonaut Sea during the summer of 2022. The study area has four large-scale oceanographic features, namely the Weddell Gyre, the Antarctic Slope Current, the southern ACC front (Williams et al., 2010), and the SB of ACC (Orsi et al., 1995; Williams et al., 2010), which are indicated by green, blue, purple, and red solid lines, respectively. There are 10 sampling sites in the area south of the SB (s-SB region) and 7 sites in the area between the SB and the sACCf (SB-sACCf region).

et al., 2010). Research has shown that between 2006 and 2020, the ACC in the Cosmonaut Sea has progressively extended southward (Zu et al., 2022), and the Antarctic Bottom Water has warmed (Aoki et al., 2020). The Southern Boundary (SB) of the Upper Circumpolar Deep Water (UCDW) distinguishes the eastward-flowing warm water from the westward-flowing Antarctic coastal water (Hunt & Hosie, 2006; Nicol et al., 2000). This SB front leads to significantly different ecosystems in its northern and southern regions with the southern region exhibiting higher primary productivity (Comiso et al., 1993; Orsi et al., 1995; Tynan, 1998). Diatoms are the predominant phytoplankton in the Cosmonaut Sea (Gomi et al., 2010; Wright & van den Enden, 2000; Wulff & Wängberg, 2004), but the dominant species differ between the south and north of the SB with *Fragilariopsis* spp. prevailing south of the SB and *D. Tenuijunctus* prevailing north of the SB (Gomi et al., 2010). Different diatom assemblages may fractionate differently (Horn et al., 2011), potentially causing variations in the isotopic effects of nitrate assimilation by phytoplankton in the northern and southern regions of the SB.

2.2. Sample Collection

Samples were collected aboard the R/V *Xuelong 2* during the 38th Chinese Antarctic Research Expedition (CHINARE) in the Cosmonaut Sea (62–67°S, 45–60°E) from 2 February 2022 to 10 March 2022 (Figure 1). A total of 17 sites were sampled throughout the water column with nitrite isotope samples collected from the upper 200 m due to insufficient concentrations for isotopic measurement at greater depths. A 10 L Niskin bottle mounted on a conductivity-temperature-depth (CTD) rosette sampler was used for sampling.

Nitrate dual isotopic samples were filtered through a 0.7 μm precombusted Whatman GF/F membrane (450°C, 4 hr) into 60 ml high-density polyethylene (HDPE) bottles. The filtrates were immediately frozen and stored onboard at −20°C. For nitrite dual isotopic samples, 5.5–6 mL of 6 mol/L NaOH was added to a 250 mL HDPE bottle to adjust the pH to >12 immediately after collection to prevent isotopic signal alteration. The samples were then stored at room temperature. Seawater for nutrient determination was filtered through a 0.45 μm cellulose acetate membrane, and the filtrates were kept frozen at −20°C until analysis. Ammonium was measured immediately onboard after sampling to avoid alteration and contamination. Temperature and salinity were recorded in situ by CTD probes.

In this study, the position of the southernmost 1.5°C isotherm in the subsurface is used to define the SB (Aoki et al., 2006; Orsi et al., 1995; Williams et al., 2010; Yamazaki et al., 2021). In the high-resolution distribution of potential temperature (not shown), the sites C4-07 and C4-03 are separated by cold water, and the 1.5°C isotherm is discontinuous between these two sites. Although the potential temperature in the subsurface water at site C4-07 is greater than 1.5°C, it is classified here as south of the SB. After this classification, the region south of the SB is denoted as s-SB, which includes 10 sites, whereas the region between the SB and the southern ACC front (sACCf) is denoted as SB-sACCf, which includes 7 sites as shown in Figure 1.

2.3. Nitrogen and Oxygen Isotopic Composition in Nitrate

The denitrification method using the strain *Pseudomonas aureofaciens* is utilized to determine the nitrogen and oxygen isotopic composition in nitrates (Casciotti et al., 2002; Sigman et al., 2001; Weigand et al., 2016). This bacteria strain lacks nitrous oxide (N_2O) reductase activity, allowing for the quantitative reduction of nitrate and nitrite to N_2O gas. Due to the lower oxygen atom fraction in nitrite compared to nitrate (3/4 vs. 5/6), the presence of nitrite can lead to an underestimation of the $\delta^{18}O$ value in nitrate even when nitrite content is less than 0.5% of the total nitrate and nitrite content (Casciotti & McIlvin, 2007; Granger & Sigman, 2009). Therefore, it is necessary to eliminate nitrite before measuring nitrate isotopes. In this study, sulfamic acid is used to remove nitrite from the samples following the method of Granger and Sigman (2009), and the pH of the treated samples is adjusted to approximately eight by adding 5 mol/L NaOH. During measurement, nitrate containing 20 nmol N is converted to N_2O by denitrifying bacteria, and the nitrogen and oxygen isotopic composition of N_2O is determined using a Thermo-Finnigan Delta^{PLUS} XP isotope ratio mass spectrometer. Four standard materials, including two international reference materials, USGS-34 ($\delta^{15}N_{air}$ = −1.8‰, $\delta^{18}O_{VSMOW}$ = −27.9‰) and IAEA-NO-3 ($\delta^{15}N_{air}$ = 4.7‰, $\delta^{18}O_{VSMOW}$ = 25.6‰), and two in-house laboratory reference materials, LAB-Mix1 ($\delta^{15}N_{air}$ = 89.3‰, $\delta^{18}O_{VSMOW}$ = −1.0‰) and LAB-Mix2 ($\delta^{15}N_{air}$ = 14.6‰, $\delta^{18}O_{VSMOW}$ = −23.1‰), are included in the samples and measured simultaneously to correct the isotopic composition of the nitrate. These two in-house laboratory reference materials consist of a mixture of two international reference materials: USGS-34 and USGS-32 ($\delta^{15}N_{air}$ = 180‰, $\delta^{18}O_{VSMOW}$ = 25.7‰). The standard deviation of replicate measurements for $\delta^{15}N$ and $\delta^{18}O$ in nitrate was 0.13 and 0.22‰ (n = 167), respectively, indicating the precision of our analyses. The nitrogen and oxygen isotopic compositions in nitrate are represented by $\delta^{15}N_{NO_3}$ and $\delta^{18}O_{NO_3}$, respectively.

2.4. Nitrogen and Oxygen Isotopic Composition in Nitrite

The azide reduction method was employed to determine the nitrogen and oxygen isotopic composition of nitrite (McIlvin & Altabet, 2005). Given that nitrite concentration in our samples is less than 2 μmol/L (Figures 3c and 3f), we transferred a subsample with a maximum injection volume of 10 ml to a 20 ml headspace vial. On the day of sample measurement, a reagent mixture with a volume ratio of 1: 1 sodium azide (2 mol/L) and acetic acid (7.8 mol/L) was prepared in advance. This mixed reagent solution was purged with high-purity helium for 1 hr to remove N_2O (Chen et al., 2023). Approximately, 0.9 ml of the purged reagent solution was added to the sample, and the reaction was allowed to proceed for 1 hr at 30°C. Subsequently, 10 mol/L NaOH was added to stop the reaction. The final product, N_2O, was analyzed using a Thermo-Finnigan Delta^{PLUS} XP isotope ratio mass spectrometer to determine the nitrogen and oxygen isotopic composition. After every 6–8 samples, a set of nitrite isotope standards, including RSIL-N23 ($\delta^{15}N_{air}$ = 3.7‰, $\delta^{18}O_{VSMOW}$ = 11.4‰), RSIL-N7373 ($\delta^{15}N_{air}$ = −79.6‰, $\delta^{18}O_{VSMOW}$ = 4.5‰), and RSIL-N10219 ($\delta^{15}N_{air}$ = 2.8‰, $\delta^{18}O_{VSMOW}$ = 88.5‰) (Casciotti et al., 2007), were measured simultaneously to calibrate the isotopic composition in the samples. The standard deviation of replicate measurements for $\delta^{15}N$ and $\delta^{18}O$ in nitrite was 0.71 and 0.78‰ (n = 65), respectively, indicating the precision of our analyses. The nitrogen and oxygen isotopic compositions in nitrite are represented by $\delta^{15}N_{NO_2}$ and $\delta^{18}O_{NO_2}$, respectively.

2.5. Physicochemical Parameters

Potential temperature and salinity were measured using the Sea-Bird 911plus CTD system with accuracies of ±0.001°C and ±0.0003 S/m, respectively.

Nitrate and nitrite concentrations were determined using the pink azo dye method and the molybdenum blue method, respectively. Ammonium concentrations were measured on board using the sodium hypobromite

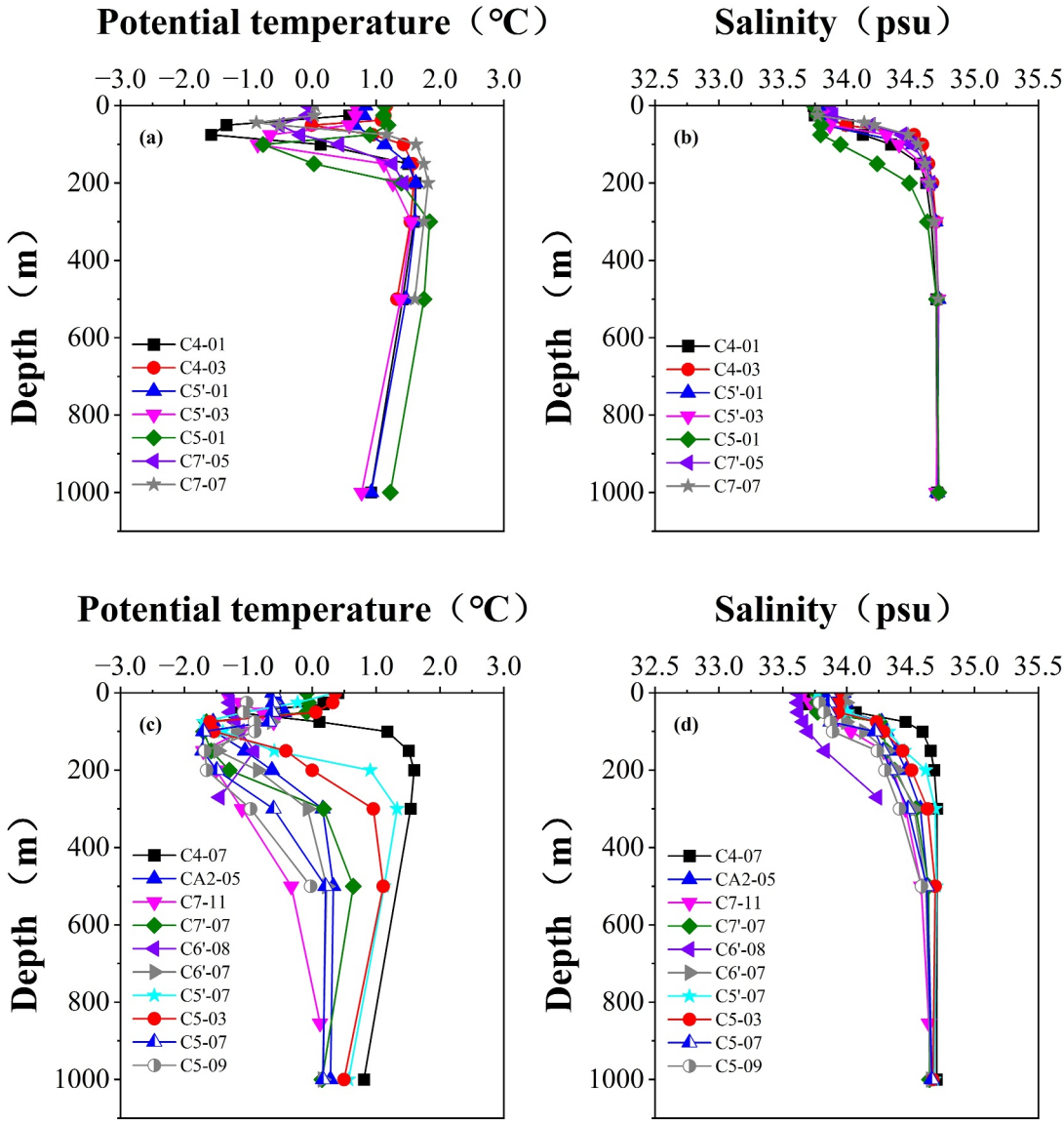

Figure 2. Profiles of potential temperature (a, c) and salinity (b, d) in the upper 1,000 m in the SB-sACCf region (a, b) and the s-SB region (c, d). Note that different stations are indicated by different symbols.

oxidation method (Huang et al., 2022). The measurement accuracies for nitrate, nitrite, and ammonium were ±1.01%, ±9.04%, and ±6.45%, respectively.

3. Results

3.1. Temperature and Salinity

The profiles of potential temperature and salinity in the Cosmonaut Sea are presented in Figure 2. The mean potential temperature in the mixed layer of the SB-sACCf region is 0.65 ± 0.45°C, higher than the −0.58 ± 0.53°C observed in the mixed layer of the s-SB region. The depth of the mixed layer in this study is determined as the shallowest depth closest to the maximum water column buoyancy frequency according to Carvalho et al. (2016) and Huang et al. (2022). The T_{min} layer, indicative of residual winter water (Altabet & Francois, 2001; Kemeny et al., 2016), is located at a depth of 50–100 m below the summer surface water. Generally, temperature increases with depth from the T_{min}, reaching a T_{max} layer at 200–500 m and then gradually decreases with further depth. Spatially, the temperature increases from T_{min} to the T_{max} layer in the SB-sACCf

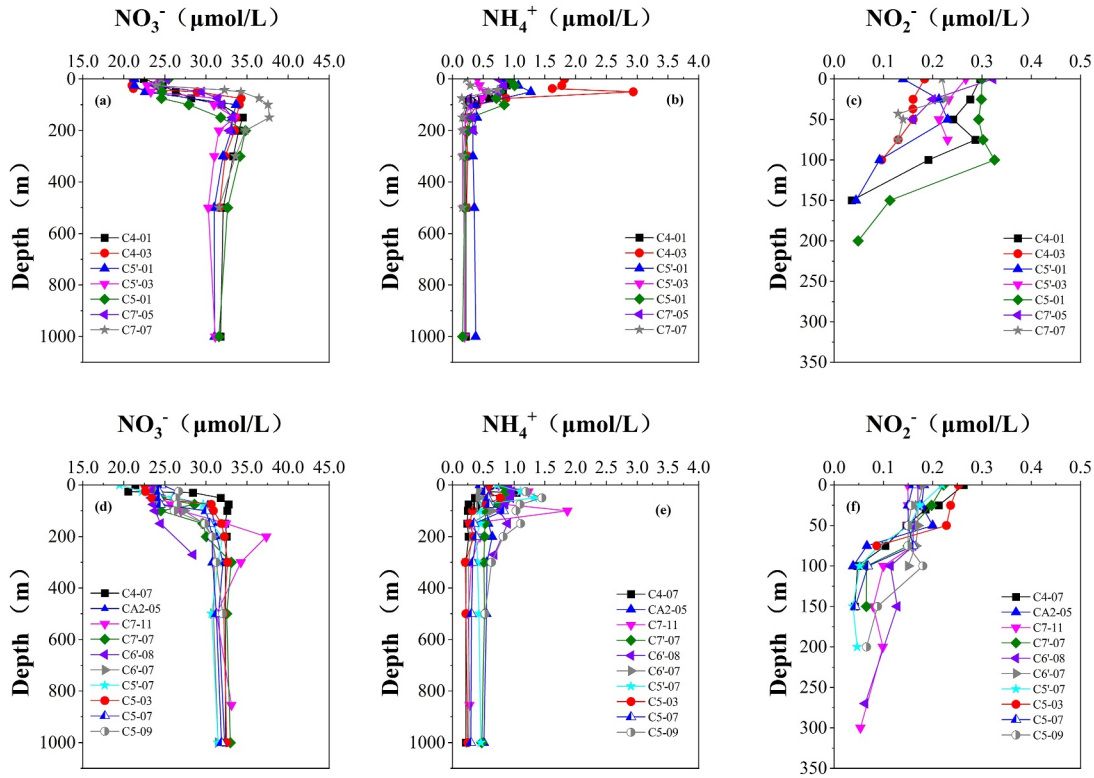

Figure 3. Profiles of NO_3^- (a, d) and NH_4^+ (b, e) in the upper 1,000 m and NO_2^- (c, f) in the upper 300 m in the SB-sACCf region (a–c) and the s-SB region (d–f). Note that different stations are indicated by different symbols.

region is significantly greater than that in the s-SB region. The potential temperature below 200 m in the SB-sACCf region averages 1.44 ± 0.29°C, which is higher than in the s-SB region (0.00 ± 0.92°C).

The average salinity in the mixed layer of the SB-sACCf region is 33.83 ± 0.07 psu, similar to the 33.83 ± 0.13 psu observed in the s-SB region. The salinity profile shows a gradual increase from the surface to 500 m after which it stabilizes. The average salinity at depths greater than 500 m in the SB-sACCf and s-SB regions is 34.71 ± 0.01 psu and 34.65 ± 0.04 psu, respectively.

3.2. Nitrate, Nitrite, and Ammonium

Nitrate concentrations in the water columns above 200 m at all sites gradually decrease toward the surface (Figures 3a and 3d). The average nitrate concentration in the mixed layer of the SB-sACCf region was 23.53 ± 2.0 μmol/L, comparable to that in the s-SB region (24.07 ± 1.64 μmol/L). At depths greater than 500 m, nitrate concentrations remain relatively uniform with averages of 31.69 ± 0.94 μmol/L in the SB-sACCf region and 31.91 ± 0.71 μmol/L in the s-SB region.

Ammonium concentrations reach a maximum at around 50 m, then decrease to 100 m, becoming relatively uniform (Figures 3b and 3e). The NH_4^+ concentration in the upper water at site C4-03 is higher than at other sites with concentrations of 1.82 μmol/L at the surface layer and 2.94 μmol/L at a depth of 50 m. Excluding site C4-03, the average NH_4^+ concentration in the mixed layer of the SB-sACCf region is 0.75 ± 0.30 μmol/L, similar to that in the s-SB region (0.79 ± 0.27 μmol/L).

The distribution of nitrite is relatively uniform in water columns above 50 m (Figures 3c and 3f). The average NO_2^- concentration in the mixed layer of the SB-sACCf region is 0.23 ± 0.06 μmol/L, slightly higher than that in the s-SB region (0.18 ± 0.03 μmol/L). Nitrite concentrations are below the detection limit at depths greater than 150 m at most sites.

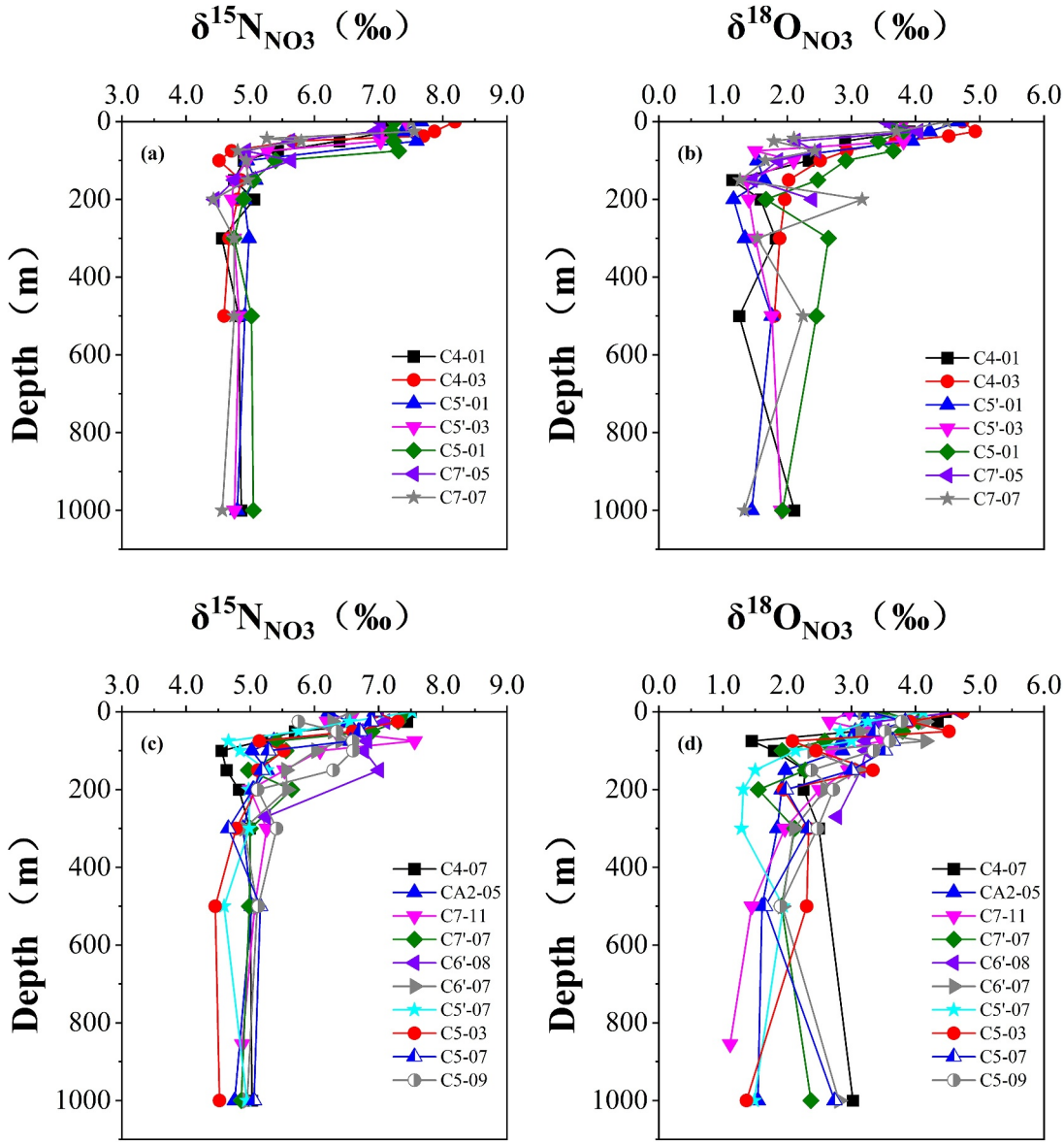

Figure 4. Profiles of $\delta^{15}N_{NO_3}$ (a, c) and $\delta^{18}O_{NO_3}$ (b, d) in the upper 1,000 m in the SB-sACCf region (a, b) and the s-SB region (c, d). Note that different stations are indicated by different symbols.

3.3. Dual Isotopes in Nitrate

The $\delta^{15}N_{NO_3}$ and $\delta^{18}O_{NO_3}$ values display an increasing trend from 200 m to the surface despite some variations in magnitude among sites (Figure 4). This isotopic variation corresponds to a decrease in nitrate concentration, reflecting the effect of phytoplankton assimilation of nitrate.

The average $\delta^{15}N_{NO_3}$ in the mixed layer of the SB-sACCf region is 7.30 ± 0.51‰, higher than that in the s-SB region (6.73 ± 0.47‰). These values exceed the surface values in OAZ (5.9 ± 0.1‰, Rafter et al., 2013) and are slightly lower than those reported for the PAZ surface (7.7 ± 1.1‰, Rafter et al., 2013). Below 500 m, $\delta^{15}N_{NO_3}$ shows slight variations with average values of 4.81 ± 0.15‰ in the SB-sACCf region and 4.91 ± 0.22‰ in the s-SB region, which are comparable to reported values for deep Southern Ocean waters (4.8 ± 0.2‰, Sigman et al., 2000; 4.7 ± 0.2‰, Rafter et al., 2013).

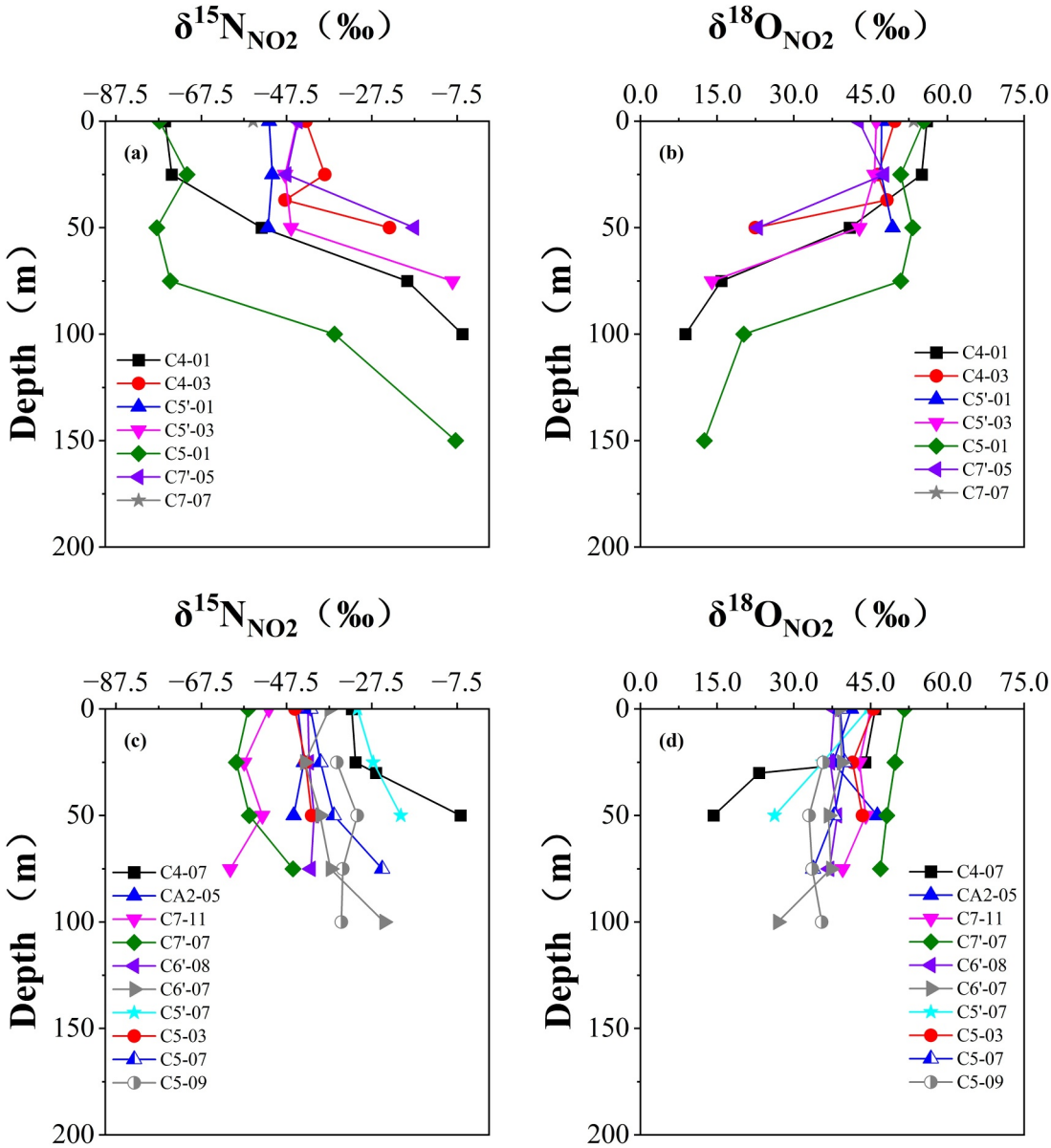

Figure 5. Profiles of $\delta^{15}N_{NO_2}$ (a, c) and $\delta^{18}O_{NO_2}$ (b, d) in the upper 1,000 m in the SB-sACCf region (a, b) and the s-SB region (c, d). Note that different stations are indicated by different symbols.

The $\delta^{18}O_{NO_3}$ values gradually increase from 200 m to the surface (Figures 4b and 4d) similar to $\delta^{15}N_{NO_3}$. The average $\delta^{18}O_{NO_3}$ in the mixed layer of the SB-sACCf region is 4.02 ± 0.45‰, slightly higher than that in the s-SB region (3.61 ± 0.54‰). Both values are higher than the surface values in OAZ (2.9 ± 0.2‰, Rafter et al., 2013) but lower than those reported for the PAZ surface (4.7 ± 1.1‰, Rafter et al., 2013). Below 500 m, $\delta^{18}O_{NO_3}$ shows slight variations with an average of 1.82 ± 0.37‰ in the SB-sACCf region and 1.87 ± 0.50‰ in the s-SB region, similar to the values (1.6 ± 0.1‰) reported by Rafter et al. (2013). The variation range of $\delta^{18}O_{NO_3}$ in deep water is greater than that of $\delta^{15}N_{NO_3}$, possibly due to larger measurement errors in $\delta^{18}O_{NO_3}$ (DiFiore et al., 2009).

3.4. Dual Isotopes in Nitrite

The vertical variation of $\delta^{15}N_{NO_2}$ at each site mirrors that of $\delta^{18}O_{NO_2}$, with $\delta^{15}N_{NO_2}$ gradually increasing with depth, whereas $\delta^{18}O_{NO_2}$ decreases with depth (Figure 5). The $\delta^{15}N_{NO_2}$ values in the upper layer of the SB-sACCf

region are generally lower than those in the s-SB region. For example, the average $\delta^{15}N_{NO_2}$ values in the surface and mixed layers of the SB-sACCf region are −56.2 ± 14.6‰ and −53.9 ± 15.3‰, respectively, whereas in the s-SB region, the values are −42.6 ± 8.4‰ and −41.3 ± 9.8‰, respectively. In contrast to $\delta^{15}N_{NO_2}$, the $\delta^{18}O_{NO_2}$ in the upper waters of the SB-sACCf region is generally higher than in the s-SB region. For instance, the average $\delta^{18}O_{NO_2}$ values in the surface and mixed layers of the SB-sACCf region are 50.1 ± 5.0‰ and 47.7 ± 7.5‰, respectively, whereas in the s-SB region, the values are 43.3 ± 4.4‰ and 40.1 ± 5.3‰, respectively.

The $\delta^{15}N_{NO_2}$ surface values obtained in this study from the Cosmonaut Sea are consistent with previous reports from the Southern Ocean, including both measured values (−90‰ to −40‰, Chen et al., 2022, 2023) and inferred values based on mass and isotopic balance (−91‰ to −41‰, Kemeny et al., 2016), but are generally lower than reported values from low-mid latitudes and the Arctic Ocean (−38–2.5‰, Buchwald et al., 2015; Casciotti et al., 2018; Chen & Chen, 2022; Liu et al., 2020). The $\delta^{18}O_{NO_2}$ values in the Cosmonaut Sea align with those reported in the Southern Ocean (35–57‰, Chen et al., 2022, 2023), but are higher than those reported from low-mid latitudes and the Arctic Ocean (from −3.3 to 23.9‰, Buchwald et al., 2015; Casciotti et al., 2018; Chen & Chen, 2022; Liu et al., 2020).

4. Discussion

4.1. Isotope Exchange Between Nitrate and Nitrite

In this section, we estimate the theoretical range of nitrogen and oxygen isotopic compositions of nitrite in the Southern Ocean based on known sources and sinks of nitrite, excluding isotopic exchange reactions. We then compare these theoretical values with the measured dual isotopic values of nitrite. If the measured values fall within the theoretical range, it suggests that conventional nitrogen cycling processes could account for our observations, suggesting minimal impact caused by isotopic exchange reactions. Conversely, if the measured values lie outside the theoretical range, it suggests other processes are influencing the isotopic composition of nitrite, thereby highlighting the role of isotopic exchange. The greater the deviation from the theoretical range, the potential impact of isotopic exchange.

4.1.1. Theoretical Range of $\delta^{15}N_{NO2}$ and $\delta^{18}O_{NO2}$ in the Conventional Nitrogen Cycle

Processes possibly affecting $\delta^{15}N_{NO_2}$ and $\delta^{18}O_{NO_2}$ in the Southern Ocean are depicted in Figure 6. The sources of nitrite include nitrate assimilation (NR) and ammonia oxidation (AO, the first step of nitrification), whereas the removal pathways include nitrite oxidation (NO, the second step of nitrification) and nitrite assimilation by phytoplankton (NA). $\delta^{15}N_{NO2}$ and $\delta^{18}O_{NO2}$ are influenced by these source and removal pathways. Additionally, $\delta^{18}O_{NO2}$ is further affected by isotopic exchange between nitrite and water ($\delta^{18}O_{H_2O}$).

When nitrite is entirely derived from nitrate assimilation, the source $\delta^{15}N_{NO2}$ value depends on $\delta^{15}N_{NO3}$ and $^{15}\varepsilon_{NR}$. With an average $\delta^{15}N_{NO3}$ of 7.2‰ in the Cosmonaut Sea and $^{15}\varepsilon_{NR}$ assumed to be 5‰ (Granger et al., 2004, 2010; Sigman et al., 1999), the $\delta^{15}N_{NO2}$ is estimated to be 2.2‰. The nitrite removal pathways also affect the $\delta^{15}N_{NO2}$. If nitrite is mainly consumed through nitrite assimilation due to $^{15}\varepsilon_{NA}$ being 1‰ (Waser et al., 1998), the $\delta^{15}N_{NO2}$ value is estimated to be 3.2‰. If nitrite is primarily consumed by oxidation to nitrate, given that $^{15}\varepsilon_{NO}$ ranges from −20‰ to −9‰ (Buchwald & Casciotti, 2010; Casciotti, 2009), the $\delta^{15}N_{NO2}$ value is estimated to be between −17.8‰ and −6.8‰.

When nitrite is entirely produced by ammonium oxidation, assessing its impact on $\delta^{15}N_{NO2}$ is more complex. The average $\delta^{15}N_{PN}$ observed in the surface waters of the Cosmonaut Sea is 0.8‰ based on data from the same voyage. Due to the preferential release of ^{14}N during particulate nitrogen degradation, $\delta^{15}N_{NH4}$ decreases by about 3‰ relative to $\delta^{15}N_{PN}$ (Buchwald & Casciotti, 2013; Lehmann et al., 2002), leading to an estimated $\delta^{15}N_{NH4}$ of about −2.2‰. Regarding the impact of NH_4^+ removal pathways on $\delta^{15}N_{NO2}$, the isotopic fractionation factor ($^{15}\varepsilon_{AO}$) of 22‰ associated with ammonia oxidation, predominantly driven by ammonia-oxidizing archaea (AOA), is fully expressed when NH_4^+ is primarily assimilated by phytoplankton (Mooshammer et al., 2020; Nishizawa et al., 2016; Santoro & Casciotti, 2011). Under these conditions, the $\delta^{15}N_{NO2}$ is estimated to be −24.2‰.

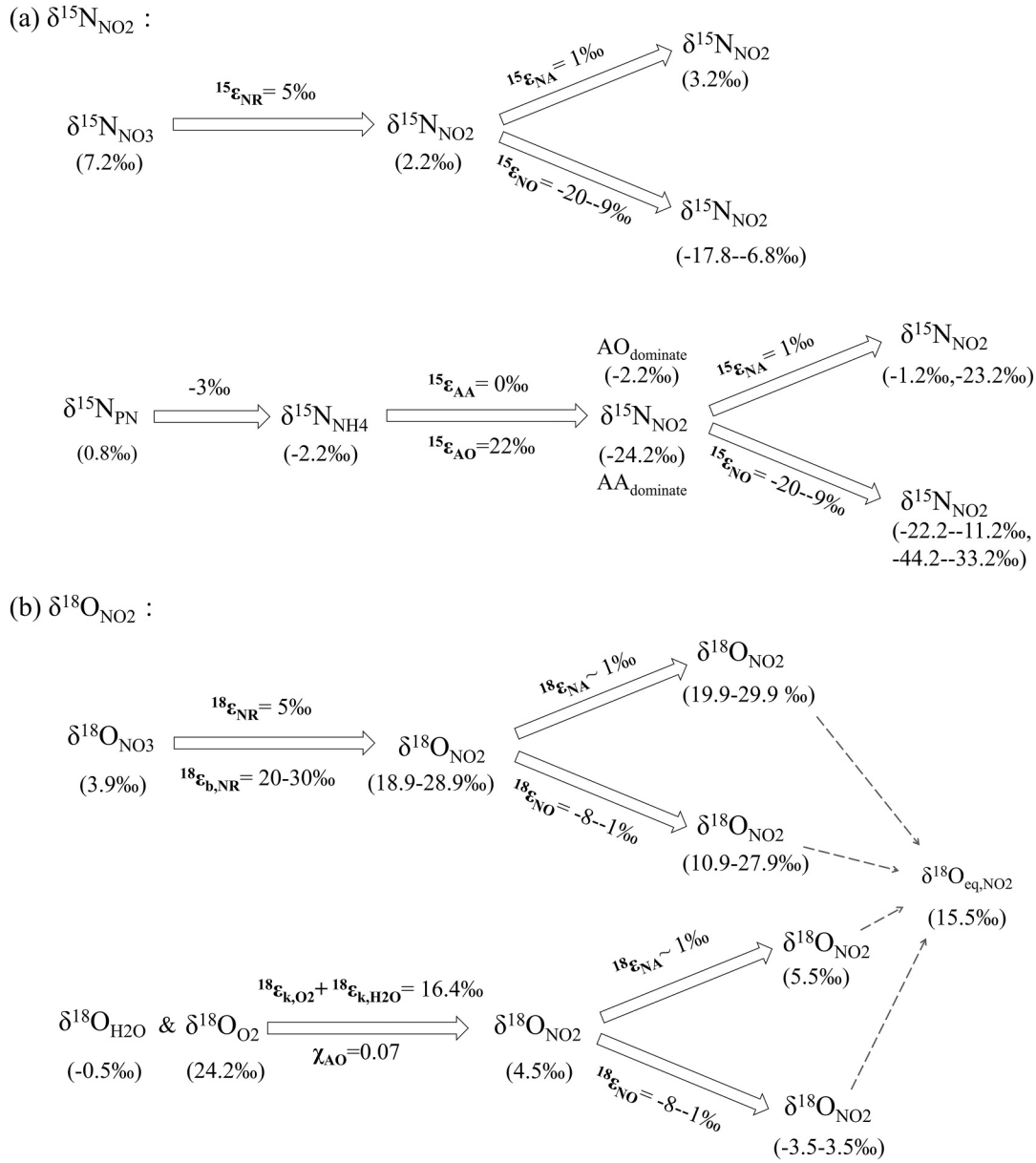

Figure 6. The ranges of $\delta^{15}N_{NO2}$ (a) and $\delta^{18}O_{NO2}$ (b) estimated based on traditional nitrogen cycling processes. These processes include two sources: nitrate assimilation (NR) and ammonium oxidation (AO), and two sinks: nitrite oxidation (NO) and nitrite assimilation (NA). The theoretical ranges of $\delta^{15}N_{NO2}$ and $\delta^{18}O_{NO2}$ are estimated using $\delta^{15}N_{NO3}$ and $\delta^{18}O_{NO3}$ (this study), $^{15}\varepsilon_{NR}$ and $^{18}\varepsilon_{NR}$ (5‰, Granger et al., 2010; Sigman et al., 1999), $^{15}\varepsilon_{NA}$ and $^{18}\varepsilon_{NA}$ (Casciotti, 2016a, 2016b; Waser et al., 1998), $^{15}\varepsilon_{NO}$ (from −20‰ to −9‰, Buchwald & Casciotti, 2010; Casciotti, 2009), $\delta^{15}N_{PN}$ (unpublished data), $^{15}\varepsilon_{AA}$ (Hoch et al., 1992; Liu et al., 2013), $^{15}\varepsilon_{AO}$ (Mooshammer et al., 2020; Nishizawa et al., 2016; Santoro & Casciotti, 2011), $^{18}\varepsilon_{b,\ NR}$ (Casciotti et al., 2007), $^{18}\varepsilon_{NO}$ (Buchwald & Casciotti, 2010), $\delta^{18}O_{H_2O}$ (−0.5‰, Chen et al., 2022), $\delta^{18}O_{O2}$ (Buchwald et al., 2012), $^{18}\varepsilon_{k,o_2}$ + $^{18}\varepsilon_{k,H_2O}$ (Buchwald et al., 2012), and χ_{AO} (Buchwald et al., 2012). The decrease in $\delta^{15}N_{NH_4}$ relative to $\delta^{15}N_{PN}$ (Buchwald & Casciotti, 2013; Lehmann et al., 2002) is also considered.

When NH_4^+ is primarily consumed by ammonia oxidation with $^{15}\varepsilon_{AA}$ around 0‰ (Hoch et al., 1992; Liu et al., 2013), the estimated $\delta^{15}N_{NO2}$ value will be −2.2‰. Therefore, considering only ammonia oxidation as the source, $\delta^{15}N_{NO2}$ will be approximately −2.2‰ or −24.2‰. Regarding the removal process, if nitrite is mainly consumed through nitrite assimilation with $^{15}\varepsilon_{NA}$ at 1‰ (Waser et al., 1998), the estimated $\delta^{15}N_{NO2}$ value will be −1.2‰ or −23.2‰. If nitrite is mainly consumed by oxidation to nitrate, with $^{15}\varepsilon_{NO}$ ranging from −20‰ to

−9‰ (Buchwald & Casciotti, 2010; Casciotti, 2009), the estimated $\delta^{15}N_{NO2}$ value will range from −22.2‰ to −11.2‰ or from −44.2‰ to −33.2‰.

From the above discussion, it can be concluded that, under the control of the conventional nitrogen cycle processes, the estimated minimum and maximum values of $\delta^{15}N_{NO2}$ are −44.2 and 2.2‰. This range is comparable to the −35–0‰ reported by Fripiat et al. (2019), which was based on calculations using equations provided by Fripiat et al. (2014).

Estimating the variation range of $\delta^{18}O_{NO_2}$ under conventional nitrogen cycle processes is more complex than estimating $\delta^{15}N_{NO_2}$ due to the oxygen isotope exchange between nitrite and water (Figure 6b). When nitrite entirely originates from nitrate assimilatory reduction, both the kinetic effect of oxygen isotope ($^{18}\varepsilon_{NR}$, 5‰; Granger et al., 2004, 2010; Karsh et al., 2012) and the O branching isotope effect ($^{18}\varepsilon_{b,NR}$, 20–30‰; Casciotti et al., 2007) affect $\delta^{18}O_{NO_2}$ and ultimately increase $\delta^{18}O_{NO_2}$. The O branching isotope effect refers to the preferential cleavage of ^{16}O-N bonds during the reaction, resulting in the production of ^{18}O-depleted H_2O and ^{18}O-enriched nitrite relative to the reacted nitrate (Casciotti, 2016a, 2016b). The measured $\delta^{18}O_{NO_3}$ value in the surface waters of the Cosmonaut Sea averages 3.9‰ from which it can be estimated that $\delta^{18}O_{NO_2}$ will range from 18.9 to 28.9‰. Regarding nitrite removal processes under this scenario, if nitrite is primarily consumed through phytoplankton assimilation, the O isotope effect for nitrite uptake remains unknown but is likely minimal similar to the nitrogen isotope fractionation associated with this process ($^{18}\varepsilon_{NA}$ ~1‰, Casciotti, 2016a, 2016b; Waser et al., 1998). Consequently, $\delta^{18}O_{NO_2}$ is estimated to remain between 19.9 and 29.9‰; if nitrite is mainly oxidized to nitrate with $^{18}\varepsilon_{NO}$ ranging from −8‰ to −1‰ (Buchwald & Casciotti, 2010), $\delta^{18}O_{NO_2}$ is estimated to be between 10.9 and 27.9‰.

When nitrite is entirely derived from ammonium oxidation, its oxygen atoms derived from both water and dissolved oxygen (Casciotti et al., 2010), and O isotope exchange between nitrite and water also occurs in the process (Casciotti et al., 2007). Assuming $\delta^{18}O_{H_2O}$ is −0.5‰ (Chen et al., 2022), $\delta^{18}O_{O_2}$ is 24.2‰, a combined oxygen incorporation isotope effect for AO ($^{18}\varepsilon_{k,O_2} + {}^{18}\varepsilon_{k,H_2O}$) of 16.4‰, and an oxygen atom exchange fraction (χ_{AO}) between nitrite and water is 0.07 (Buchwald et al., 2012), $\delta^{18}O_{NO_2}$ is estimated to be approximately 4.5‰ based on the equation provided by Buchwald and Casciotti (2013). If this nitrite is mainly assimilated by phytoplankton, $\delta^{18}O_{NO_2}$ value is estimated to 5.5‰. If these nitrite are primarily oxidized to nitrate, given that $^{18}\varepsilon_{NO}$ ranges from −8‰ to −1‰ (Buchwald & Casciotti, 2010), $\delta^{18}O_{NO2}$ value will range from −3.5 to 3.5‰.

Based on the above discussion, the estimated range of $\delta^{18}O_{NO_2}$ under traditional nitrogen cycle processes spans from a maximum of 29.9‰ to a minimum of −3.5‰, respectively. In addition to these biological processes, nitrite and water undergo oxygen isotope exchange (Buchwald & Casciotti, 2013; Casciotti et al., 2007). According to the temperature-dependent equilibrium isotope effect formula for abiotic oxygen atoms exchange between nitrite and H_2O expressed as $^{18}\varepsilon_{eq} = -0.12*T(K) + 48.79$, $\delta^{18}O_{NO_2}$ is estimated to be 15.5‰ (Buchwald & Casciotti, 2013; Casciotti et al., 2007) based our in situ temperature. If the biological turnover rate of nitrite exceeds the rate of abiotic oxygen isotope exchange, $\delta^{18}O_{NO_2}$ will stabilize between −3.5 and 29.9‰. Otherwise, it will converge to the equilibrium value of 15.5‰ over weeks to months, reflecting the timescale of O isotope exchange between nitrite and water (Buchwald & Casciotti, 2013; Chen, 2021; Chen & Chen, 2022).

4.1.2. Evidence for Isotope Exchange Between Nitrate and Nitrite

From the discussion in Section 4.1.1, we know that the expected minimum $\delta^{15}N_{NO_2}$ value for the conventional nitrogen cycle processes is −44.2‰, and the maximum $\delta^{18}O_{NO_2}$ value is 29.9‰, which do not account for our observations in the Cosmonaut Sea. The $\delta^{15}N_{NO_2}$ values in the surface water of the SB-sACCf region range from −77.3‰ to −43.0‰ with an average of −56.2 ± 14.6‰, and the $\delta^{18}O_{NO2}$ values range from 42.7 to 56.0‰ with an average of 50.1 ± 5.0‰ (see Section 3.4). In the surface water of the s-SB region, $\delta^{15}N_{NO_2}$ values range from −56.5‰ to −30.9‰ with an average of −43.4 ± 8.3‰, and the $\delta^{18}O_{NO_2}$ values range from 37.9 to 51.6‰ with an average of 43.3 ± 4.4‰ (see Section 3.4). The $\delta^{15}N_{NO_2}$ values are generally lower than the theoretically minimum, whereas the $\delta^{18}O_{NO_2}$ values are higher than the theoretically maximum, suggesting that other processes influence the dual isotopic composition of nitrite. Recent studies have shown that there is an exchange of nitrogen and oxygen between nitrate and nitrite (Chen et al., 2022; Fripiat et al., 2019; Kemeny et al., 2016). Kemeny

et al. (2016) estimated the NXR-mediated nitrogen isotope equilibrium of this exchange reaction to be between −69.2‰ and −59.9‰ using a molecular vibration frequency method. The unusually low $\delta^{15}N_{NO_2}$ values observed in the Cosmonaut Sea can be explained by the large NXR-mediated nitrogen isotope effect of the isotope exchange between nitrate and nitrite. Similarly, the unusually high $\delta^{18}O_{NO_2}$ values can be attributed to the substantial NXR-mediated oxygen isotope effect (37.6 ± 3.5‰, Chen et al., 2022), which arises from the isotopic exchange reaction between nitrite and nitrate. This value was estimated by assuming isotopic equilibrium between nitrite and nitrate, followed by calculating the NXR-mediated equilibrium isotope effect from the isotopic differences between the two species. Following the methodology established by Chen et al. (2022), we assumed that nitrate and nitrite had reached isotopic equilibrium during the sampling. By averaging the nitrogen and oxygen isotopic compositions of nitrate and nitrite in the surface layer and calculating their isotopic differences, we determined the NXR-mediated equilibrium fractionation factors for both nitrogen and oxygen. The NXR-mediated nitrogen isotope equilibrium value in the Cosmonaut Sea was −55.7 ± 13.1‰, which aligns well with previously reported values ranging from −69.2‰ to −53.9‰ (Casciotti, 2009; Chen et al., 2022; Kemeny et al., 2016). Similarly, the NXR-mediated oxygen isotope equilibrium value was 42.4 ± 5.7‰, closely aligning with the 37.6 ± 3.5‰ reported by Chen et al. (2022) for the Amundsen Sea. The relatively lower NXR-mediated oxygen isotope equilibrium value may be attributed to the incorporation of ^{18}O-depleted atoms from ambient H_2O (Chen et al., 2022).

4.2. Does Nitrate-Nitrite Isotope Exchange Impact Isotope Effect Estimates in Nitrate Assimilation?

Our evidence from $\delta^{15}N_{NO_2}$ and $\delta^{18}O_{NO_2}$ suggests that isotope exchange occurs between nitrate and nitrite in the Cosmonaut Sea, which enriches ^{15}N and depletes ^{18}O in nitrate. However, its impact on estimating the isotope effect of nitrate assimilation, particularly for oxygen, remains unclear. We compared the isotope effect of nitrate assimilation estimated from the traditional $\delta^{15}N_{NO_3}/\delta^{18}O_{NO_3}$ versus ln[NO_3] relationship ($^{15}\varepsilon_{NO3\text{-}only}$ and $^{18}\varepsilon_{NO3\text{-}only}$) with estimates that account for nitrate-nitrite isotope exchange. Previous studies indicate that although isotope exchange alters the individual isotopic compositions of nitrate and nitrite, it does not change the combined isotopic signature of the NO_3^- + NO_2^- pool (Fripiat et al., 2019; Kemeny et al., 2016). By treating NO_3^- and NO_2^- as a combined pool, the apparent $\delta^{15}N$ and $\delta^{18}O$ values were calculated using an isotope mass balance approach. The isotope effect ($^{15}\varepsilon_{NO_3+NO_2}$ and $^{18}\varepsilon_{NO_3+NO_2}$) was determined using $^{15}N_{NO_3+NO_2}/^{18}O_{NO_3+NO_2}$ versus ln[NO_3 + NO_2]. Consequently, $^{15}\varepsilon_{NO_3+NO_2}$ and $^{18}\varepsilon_{NO_3+NO_2}$ reflect the isotope effect of phytoplankton assimilating nitrate, unaffected by nitrate-nitrite isotope exchange, a method we term the N + N method. We compared $^{15}\varepsilon_{NO_3-only}$ (or $^{18}\varepsilon_{NO_3-only}$) with $^{15}\varepsilon_{NO_3+NO_2}$ (or $^{18}\varepsilon_{NO_3+NO_2}$) to evaluate whether nitrate-nitrite isotope exchange influences the estimated isotope effects during nitrate assimilation. Additionally, we calculated the isotope effects in nitrate assimilation for both the SB-sACCf region and the s-SB region to observe potential differences between these two areas. To mitigate the dilution effect of sea ice and glacier meltwater, nitrate and nitrite concentrations were normalized to a salinity of 35 psu (Henley et al., 2017).

In both the SB-sACCf and s-SB regions, the measured values of $\delta^{15}N_{NO_3}$ and $\delta^{18}O_{NO_3}$ in Antarctic Surface Water (AASW), characterized by the surface mixed layer and T_{min} layer, exhibit a significant linear negative correlation with ln[NO_3], consistent with the Rayleigh model. The slopes of this fitted relationship yield $^{15}\varepsilon_{NO_3-only}$ and $^{18}\varepsilon_{NO_3-only}$ values for the SB-sACCf region of 6.4 ± 0.6‰ and 6.4 ± 0.5‰, respectively (Figures 7a and 7c). The $^{15}\varepsilon_{NO_3-only}$ value in the SB-sACCf region of the Cosmonaut Sea is lower than the reported values for the SAZ (8–10‰, DiFiore et al., 2006). Similarly, in the s-SB region, the $^{15}\varepsilon_{NO_3-only}$ and $^{18}\varepsilon_{NO_3-only}$ values are 5.4 ± 0.4‰ and 4.2 ± 0.5‰, respectively (Figures 8a and 8c).

In both the SB-sACCf and s-SB regions, the $\delta^{15}N_{NO_3+NO_2}$ and $\delta^{18}O_{NO_3+NO_2}$ in AASW exhibit a significant negative correlation with ln[NO_3 + NO_2] (Figures 7 and 8) consistent with previous observations in the Southern Ocean (Fripiat et al., 2019; Kemeny et al., 2016). The $^{15}\varepsilon_{NO_3+NO_2}$ value estimated using the N + N method in the SB-sACCf region is 5.2 ± 0.6‰, which is close to the reported value for the PAZ (5.0 ± 0.7‰, DiFiore et al., 2009). The corresponding $^{18}\varepsilon_{NO_3+NO_2}$ value is 7.4 ± 0.6‰ (Figures 7b and 7d). In comparison, the values in the s-SB region for $^{15}\varepsilon_{NO_3+NO_2}$ and $^{18}\varepsilon_{NO_3+NO_2}$ are 4.3 ± 0.4‰ and 5.3 ± 0.6‰, respectively (Figures 8b and 8d).

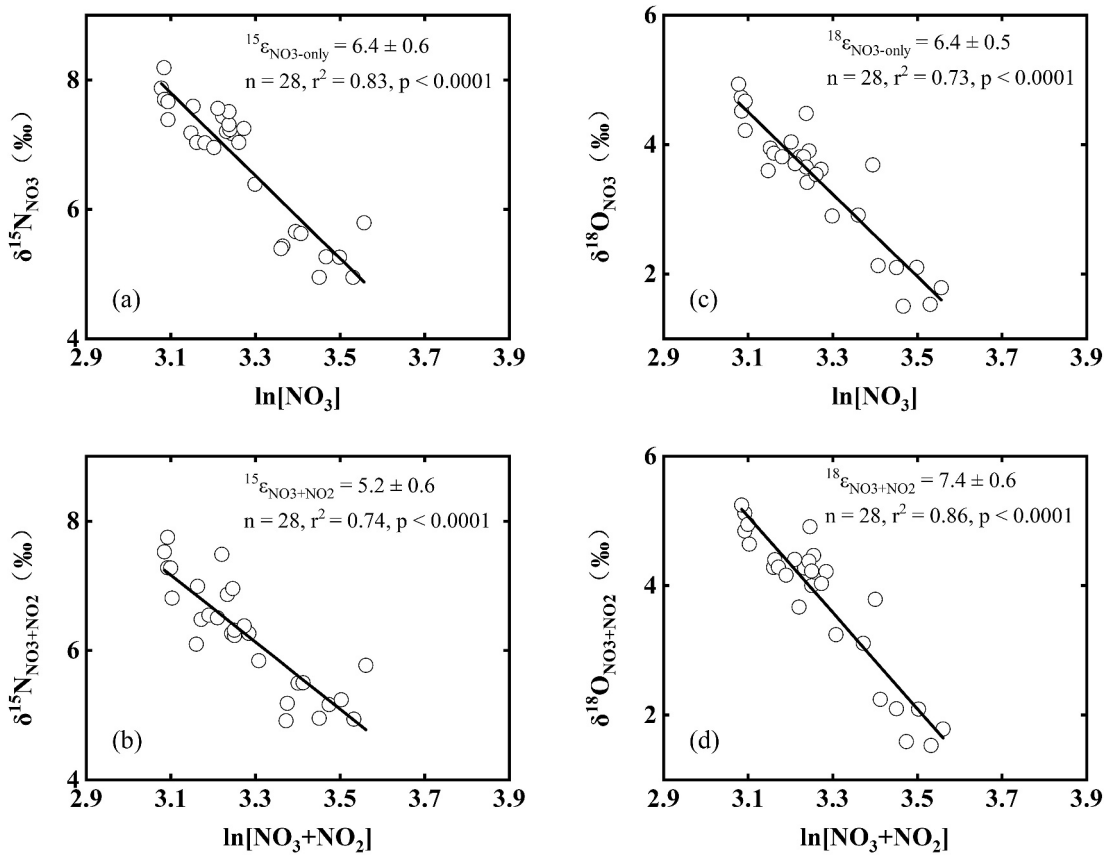

Figure 7. Rayleigh plot of nitrogen and oxygen isotopic composition in nitrate from the SB-sACCf region (a. $\delta^{15}N_{NO_3}$; b. $\delta^{15}N_{NO_3+NO_2}$; c. $\delta^{18}O_{NO_3}$; d. $\delta^{18}O_{NO_3+NO_2}$). The subplots (a and b) in the left column represent nitrogen isotopic compositions; the subplots (c and d) in the right column represent oxygen isotopic compositions.

The comparison of $^{15}\varepsilon_{NO_3-only}$ (or $^{18}\varepsilon_{NO_3-only}$) with $^{15}\varepsilon_{NO_3+NO_2}$ (or $^{18}\varepsilon_{NO_3+NO_2}$) reveals significant differences between them in both the SB-sACCf and s-SB regions as determined by the probability *t*-test ($P < 0.05$). This indicates that isotope exchange between nitrate and nitrite affects the estimated values of the isotope effect in nitrate assimilation for both nitrogen and oxygen. Similar to our findings, Fripiat et al. (2019) demonstrated, through nitrogen and oxygen isotope measurements of both NO_3^--only and the NO_3^- + NO_2^- system, that the estimated nitrogen isotope effect from the NO_3^- + NO_2^- system was significantly lower than that obtained from the NO_3^--only system. However, in contrast to our findings, Fripiat et al. (2019) did not observe the influence of oxygen isotope exchange reactions on the oxygen isotope effect. Although nitrite constitutes only 0.8% of the average nitrate concentration in the mixed layer, its extremely low $\delta^{15}N$ and high $\delta^{18}O$ relative to nitrate also alter the nitrogen and oxygen isotopic composition of the NO_3^- + NO_2^- system, particularly in the upper layers. This results in a maximum difference of 1.1‰ in $\delta^{15}N$ and 0.68‰ in $\delta^{18}O$ between the NO_3^- + NO_2^- and NO_3^--only systems. The difference between $\delta^{15}N_{NO_3+NO_2}$ and $\delta^{15}N_{NO_3}$ is most pronounced at the surface (0.44 ± 0.22‰) but gradually decreases with depth reaching 0.31 ± 0.16‰ at 100 m, where the WW layer is typically located. Similarly, the difference between $\delta^{18}O_{NO_3+NO_2}$ and $\delta^{18}O_{NO_3}$ is larger at the surface (0.40 ± 0.14‰) and diminishes with increasing depth, dropping to 0.18 ± 0.04‰ at 100 m. The progressively decreasing differences with depths may impact the apparent $^{15}\varepsilon$, resulting in $^{15}\varepsilon_{NO_3-only} > {}^{15}\varepsilon_{NO_3+NO_2}$ and $^{18}\varepsilon_{NO_3+NO_2} > {}^{18}\varepsilon_{NO_3-only}$. The oxygen isotope dynamics are more complex than those of nitrogen due to the incorporation of O atoms from ambient H_2O influence fractionation factors derived from linear regression of the Rayleigh model.

Using winter water (WW) as the initial source (Kemeny et al., 2016), we estimated the isotope effect for each station individually, excluding station C4-01 due to identified issues with the T_{min} layer data. In contrast to the findings of Kemeny et al. (2016) and Fripiat et al. (2019), our results indicated that the ε values for the NO_3^- + NO_2^- system were predominantly clustered near the 1: 1 line (Figure 9a). This observation aligns with

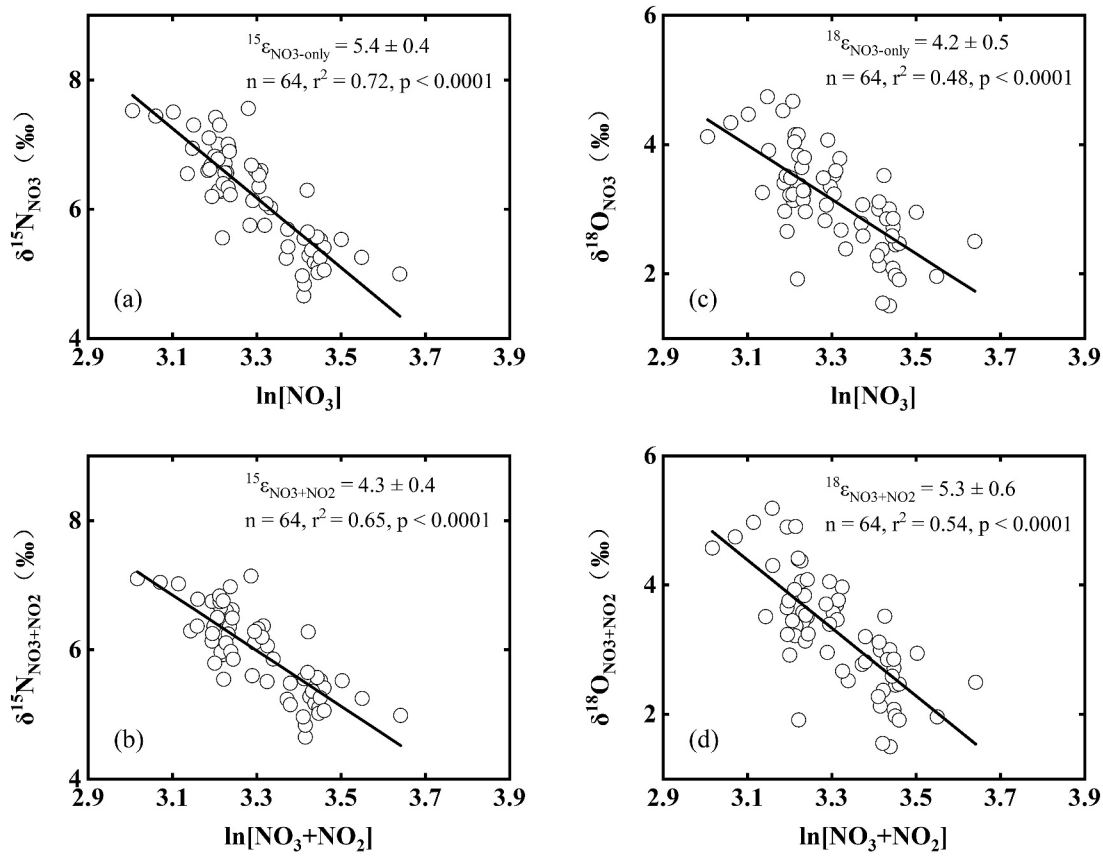

Figure 8. Rayleigh plot of nitrogen and oxygen isotopic composition in nitrate from the s-SB region (a. $\delta^{15}N_{NO_3}$; b. $\delta^{15}N_{NO_3+NO_2}$; c. $\delta^{18}O_{NO_3}$; d. $\delta^{18}O_{NO_3+NO_2}$). The subplots (a and b) in the left column represent nitrogen isotopic compositions; the subplots (c and d) in the right column represent oxygen isotopic compositions.

the fact that NO_3^- + NO_2^- samples correspond with the 1: 1 line in $\delta^{18}O$ versus $\delta^{15}N$ (Figure 11), which is expected if nitrate assimilation operates independently. These results further support the idea that the NO_3^- + NO_2^- system more accurately represents the "true" isotope effect associated with nitrate assimilation (Fripiat et al., 2019).

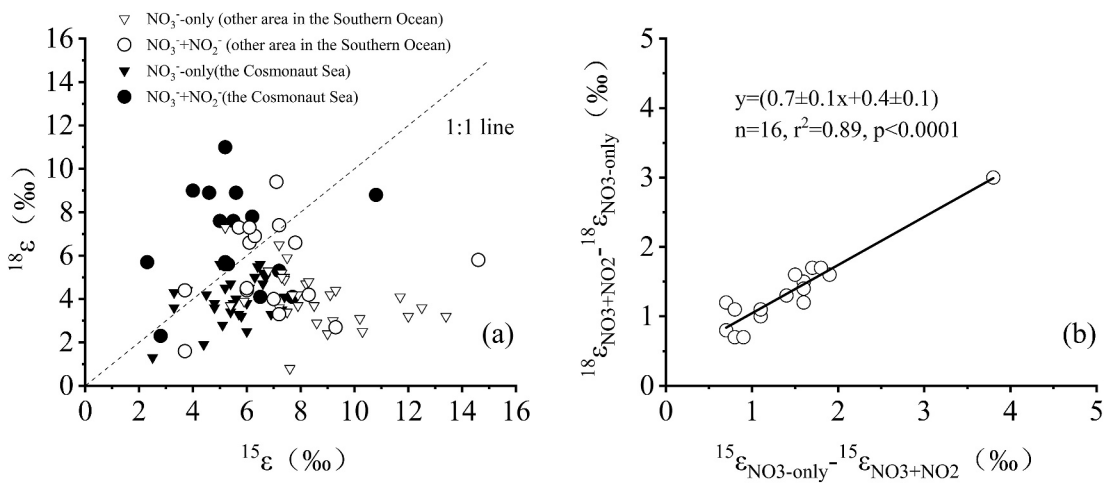

Figure 9. (a) Relationship between $^{18}\varepsilon$ and $^{15}\varepsilon$ for NO_3^- + NO_2^- (filled circles: this study; filled inverted triangles: other area in the Southern Ocean (Fripiat et al., 2019)) and NO_3^--only (open circles: our study; open inverted triangles: other area in the Southern Ocean (Fripiat et al., 2019)). (b) Relationship between $^{15}\varepsilon_{NO_3-only} - {}^{15}\varepsilon_{NO_3+NO_2}$ (the apparent intensity of isotope exchange reactions) and $^{18}\varepsilon_{NO_3+NO_2} - {}^{18}\varepsilon_{NO_3-only}$.

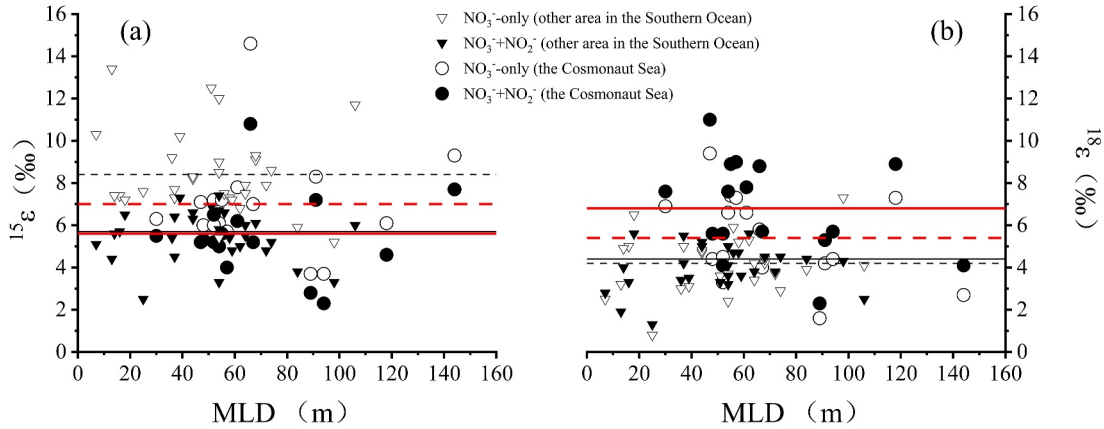

Figure 10. Relationship between $^{15}\varepsilon$ (a) and $^{18}\varepsilon$ (b) and MLD for $NO_3^- + NO_2^-$ system (filled circles: this study; filled inverted triangles: other regions in the Southern Ocean (Fripiat et al., 2019)) and NO_3^--only system (open circles: our study; open inverted triangles: other regions in the Southern Ocean (Fripiat et al., 2019)). The solid red line and dashed red line represent the average values of $^{15}\varepsilon_{NO_3+NO_2}$ (5.6‰) and $^{18}\varepsilon_{NO_3+NO_2}$ (6.8‰) for $NO_3^- + NO_2^-$ system as well as the average values of $^{15}\varepsilon_{NO_3-only}$ (7.0‰) and $^{18}\varepsilon_{NO_3-only}$ (5.4‰) for NO_3^--only system in the Cosmonaut Sea. The solid black line indicates the average values of $^{15}\varepsilon_{NO_3+NO_2}$ (5.7‰) and $^{18}\varepsilon_{NO_3-only}$ (4.4‰) for $NO_3^- + NO_2^-$ system, whereas the dashed black lines denote the average values of $^{15}\varepsilon_{NO_3-only}$ (8.4‰) and $^{18}\varepsilon_{NO_3-only}$ (4.2‰) for NO_3^--only system in other regions of the Southern Ocean.

Previous studies have indicated that the differences in $^{15}\varepsilon$ between the $NO_3^- + NO_2^-$ system and the NO_3^--only system could serve as indicators of the degree of isotope exchange reactions (Fripiat et al., 2019; Kemeny et al., 2016). We also observed a significant linear relationship between the differences in $^{15}\varepsilon$ and $^{18}\varepsilon$ for both the $NO_3^- + NO_2^-$ system and the NO_3^--only system (Figure 9b). This finding implies that the differences in $^{18}\varepsilon$ may, to some extent, reflect the intensity of oxygen isotopic exchange. Furthermore, the slope of this linear relationship was 0.7, which is less than 1, likely due to the influence of oxygen isotopic exchange with water within the $NO_3^- + NO_2^-$ system. Assuming that nitrate and nitrite were already in isotopic exchange equilibrium at the time of sampling, as discussed in Section 4.1.2, and applying the known NXR-mediated nitrogen isotope equilibrium value (−55.7 ± 13.1‰), we calculated the NXR-mediated oxygen isotope equilibrium value to be 39.0 ± 10.7‰. This result closely aligns with the value obtained in Section 4.1.2 (42.4 ± 5.7‰) using the method of Chen et al. (2022), underscoring the reliability of the linear relationship in estimating isotopic fractionation factors.

4.3. Difference in ε Values between the SB-sACCf and s-SB Regions and Its Reasons

The spatial variation of ε values in the Cosmonaut Sea shows significantly lower ε in the s-SB region compared to the SB-sACCf region for both nitrogen and oxygen, as determined by the probability *t*-test ($p < 0.05$) (Figures 7 and 8). The observed decrease in fractionation factors with latitude aligns with the findings of DiFiore et al. (2010), whose study revealed a strong positive linear relationship between $^{15}\varepsilon$ values and mixed layer depth, attributing primarily to light availability. Conversely, the study by Fripiat et al. (2019) found no significant relationship between fractionation factors and MLDs. Our results at each station support the viewpoint that there is no correlation (Figure 10). Furthermore, the MLD in the s-SB region (80.5 ± 30.0 m) is significantly deeper than that in the SB-sACCf region ($p < 0.05$), suggesting that factors beyond light availability may account for the lower $^{15}\varepsilon$ values observed in the s-SB region. Additionally, the fractionation factors at individual stations indicate that the average $^{15}\varepsilon_{NO_3+NO_2}$ value for the $NO_3^- + NO_2^-$ system is 5.6‰ consistent with previous reports (5.7‰, Fripiat et al., 2019). In contrast, the oxygen fractionation factor exhibits a different trend with the average $^{18}\varepsilon_{NO_3-only}$ value for the NO_3^--only system (5.4‰) being lower than the $^{18}\varepsilon_{NO_3+NO_2}$ for the $NO_3^- + NO_2^-$ system (6.8‰). In the Cosmonaut Sea, the average values for the $NO_3^- + NO_2^-$ system and NO_3^--only system are $^{15}\varepsilon_{NO3+NO2}$ (5.6‰), $^{18}\varepsilon_{NO3+NO2}$ (6.8‰) and $^{15}\varepsilon_{NO_3-only}$ (7.0‰), $^{18}\varepsilon_{NO_3-only}$ (5.4‰), respectively. In other regions of the Southern Ocean, the averages are $^{15}\varepsilon_{NO_3+NO_2}$ (5.7‰), $^{18}\varepsilon_{NO_3+NO_2}$ (4.4‰) and $^{15}\varepsilon_{NO_3-only}$ (8.4‰), $^{18}\varepsilon_{NO_3-only}$ (4.2‰).

Nitrification tends to introduce low-$\delta^{15}N$ nitrate into the mixed layer while reducing the apparent fractionation factor (Henley et al., 2018; Sigman et al., 1999; Smart et al., 2015). To evaluate the influence of nitrification on ε

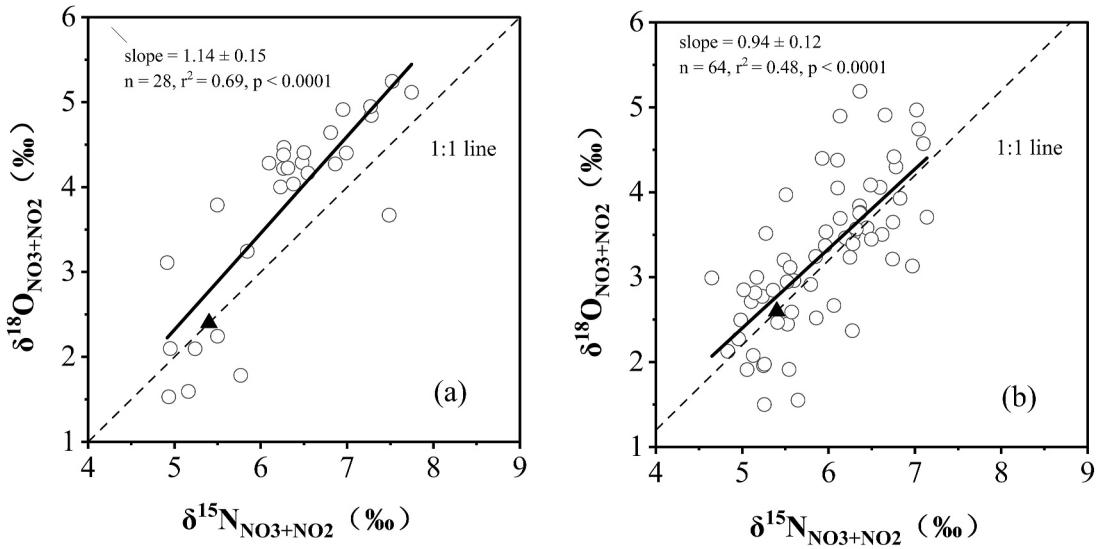

Figure 11. (a) Relationship between $\delta^{18}O$ and $\delta^{15}N$ for $NO_3^- + NO_2^-$ (a) in the SB-sACCf and (b) in the s-SB region. Filled triangles mark WW averages, and the black dotted line shows the 1:1 ratio through the WW average point.

estimation, we analyzed the isotopic distributions of nitrogen and oxygen in the $NO_3^- + NO_2^-$ system across both regions. The results show that the $\delta^{18}O$ and $\delta^{15}N$ distributions vary in a 1:1 ratio, corresponding to the characteristics of the nitrate assimilation process, particularly in the s-SB region (Figure 11). In Section 4.2, our results also show that ε values for the $NO_3^- + NO_2^-$ system near the 1:1 line (Figure 9a), which aligns with the expectation that nitrate assimilation dominates, suggesting that the impact of nitrification on ε can be temporarily overlooked.

Iron plays a crucial role in primary production in the Southern Ocean. Under both iron-limited and iron-replete conditions, phytoplankton exhibit different △Si/△N uptake ratios. Specifically, △Si/△N is calculated as $(Si_{WW} - nSi_{obs})/(N_{WW} - nN_{obs})$, where Si_{WW} and N_{WW} represent the concentrations of silicate and nitrate in the WW, respectively, and nSi_{obs} and nN_{obs} are the silicate and nitrate concentrations normalized to the salinity of the WW. It was observed that the uptake ratio is higher under iron-limited conditions (Takeda, 1998; Tamura et al., 2023). ΔSi/ΔN can also vary due to differences in phytoplankton assemblages (Arrigo et al., 1999). However, in our study region, *Phaeocystis antarctica* was the dominant species in the surface waters (Yang et al., 2022). Therefore, due to the lack of iron concentration measurements, we assume that △Si/△N can still serve as an indicator of iron limitation levels to some extent. We calculated the ΔSi/ΔN ratios in the mixed layer at each site using water masses with potential temperatures below −1.5°C as representatives of the initial winter conditions for both regions. The results indicate that the △Si/△N ratio in the SB-sACCf region is significantly higher than that in the s-SB region, suggesting greater iron limitation in the SB-sACCf region. In contrast, the higher iron availability in the s-SB region may be attributed to inputs from sea ice, glacial meltwater, and continental shelves (Lannuzel et al., 2010; Nicol et al., 2000; Qi et al., 2024; Sedwick et al., 2000; Tagliabue et al., 2009). Studies have shown that increased environmental iron reduces the isotope effect of nitrate assimilation by decreasing nitrate efflux, which results from enhanced intracellular nitrate reduction under iron-replete conditions (Karsh et al., 2003, 2012; Li et al., 2023; Smith et al., 2021; Takeda, 1998). Additionally, we observed a strong positive linear correlation between $^{18}\varepsilon_{NO_3+NO_2}$ and △Si/△N ($p < 0.05$), whereas $^{15}\varepsilon$ did not exhibit the same trend ($p > 0.05$) (Figure 12). This finding between $^{18}\varepsilon_{NO_3+NO_2}$ and △Si/△N reinforces the conclusion that iron availability contributes to the lower ε values in the s-SB region compared to the SB-sACCf region, particularly reflected in the oxygen isotope effect.

Additionally, we considered the impact of phytoplankton composition and abundance on fractionation factors. Different phytoplankton species exhibit distinct isotope effects during nitrate assimilation (Granger et al., 2004, 2010; Montoya & McCarthy, 1995). Although *Phaeocystis antarctica* and *Fragilariopsis kerguelensis* display lower fractionation factors compared to other diatom species (Granger et al., 2004, 2010; Horn et al., 2011; Montoya & McCarthy, 1995), their relative abundances within phytoplankton communities show no significant

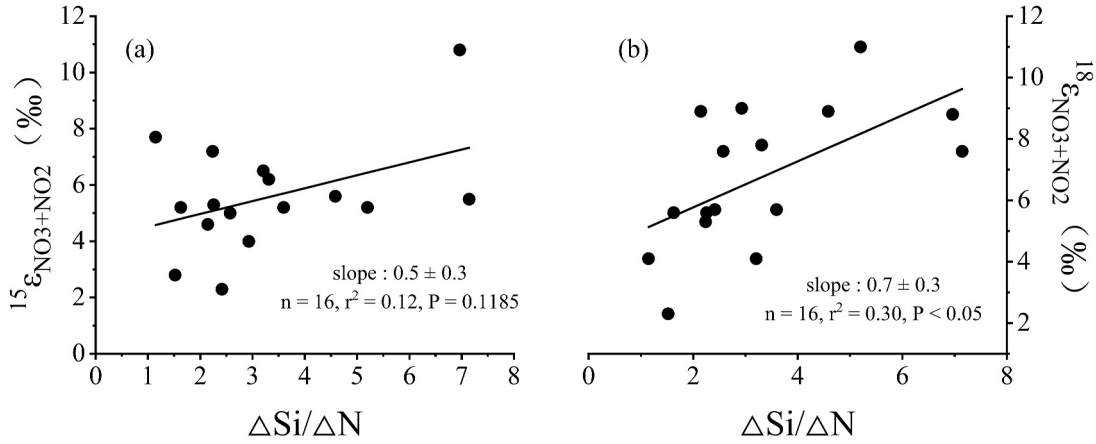

Figure 12. (a) Relationship between $^{15}\varepsilon_{NO_3+NO_2}$ and △Si/△N, and (b) Relationship between $^{18}\varepsilon_{NO_3+NO_2}$ and △Si/△N.

difference between the two regions ($P > 0.05$). Therefore, phytoplankton composition is also unlikely to be a major factor influencing the north-south variation in fractionation factors. Other potential factors, such as vertical mixing, may influence regional differences in fractionation factors. Vertical mixing would introduce low-$\delta^{15}N$ nitrate from deeper layers into the summer mixed layer potentially affecting ε estimates (Sigman et al., 1999). However, this process is spatially limited, intermittent, and more pronounced in winter. During our sampling period (summer) in the Antarctic Zone, the influence of vertical mixing appears to be minimal (Sigman et al., 1999). Additionally, nitrate concentrations and isotopic signatures in Winter Water below the summer mixed layer showed no significant differences between the two regions, likely due to both regions deriving their deep water from LCDW. Therefore, vertical mixing is unlikely to be the primary driver of the observed fractionation differences.

5. Conclusions

The analysis of the dual isotopic composition of nitrate and nitrite in the Cosmonaut Sea indicates that isotopic exchange between nitrate and nitrite results in unusually low $\delta^{15}N$ values and unusually high $\delta^{18}O$ values of nitrite in the mixed layer while exerting relatively little influence on the dual isotopic composition of nitrate. Utilizing the Rayleigh model to calculate the isotope effect of nitrate assimilation by phytoplankton, both with and without accounting for nitrate-nitrite isotopic exchange, demonstrates that this exchange significantly impacts the estimated isotope effects for both nitrogen and oxygen. Furthermore, the nitrogen and oxygen isotope effects of nitrate assimilation in the Cosmonaut Sea exhibit considerable spatial variation with values in the s-SB region being lower than those in the SB-sACCf region. This variability is primarily associated with environmental iron availability as indicated by the positive correlation between $^{18}\varepsilon_{NO_3+NO_2}$ and △Si/△N.

Conflict of Interest

The authors declare no conflicts of interest relevant to this study.

Data Availability Statement

The data used in the manuscript are available through Mendeley Data at https://doi.org/10.17632/nzzdwrjnxs.1. Figures were made with OriginPro 2025 (https://www.originlab.com/). The map was created through ocean date view (Schlitzer, R., Ocean Date View, http://odv.awi.de).

Acknowledgments
We gratefully acknowledge the support of the captain and crew of the R/V *Xuelong 2* during our sampling. This research was funded by the Polar Research Institute of China (IRASCC 02-01-01 and IRASCC 01-01-02C) and the National Natural Science Foundation of China (No. 41721005).

References

Altabet, M. A., & Francois, R. (1994). Sedimentary nitrogen isotopic ratio as a recorder for surface ocean nitrate utilization. *Global Biogeochemical Cycles*, *8*(1), 103–116. https://doi.org/10.1029/93GB03396

Altabet, M. A., & Francois, R. (2001). Nitrogen isotope biogeochemistry of the Antarctic polar frontal zone at 170°W. *Deep - Sea Research Part II: Topical Studies in Oceanography*, *48*(19–20), 4247–4273. https://doi.org/10.1016/S0967-0645(01)00088-1

Aoki, S., Katsumata, K., Hamaguchi, M., Noda, A., Kitade, Y., Shimada, K., et al. (2020). Freshening of Antarctic bottom water off Cape Darnley, east Antarctica. *Journal of Geophysical Research: Oceans*, *125*(8), e2020JC016374. https://doi.org/10.1029/2020JC016374

Aoki, S., Rintoul, S. R., Hasumoto, H., & Kinoshita, H. (2006). Frontal positions and mixed layer evolution in the Seasonal Ice Zone along 140°E in 2001/02. *Polar Bioscience*, *20*, 1–20. https://doi.org/10.15094/00006254

Arrigo, K. R., Robinson, D. H., Worthen, D. L., Dunbar, R. B., DiTullio, G. R., VanWoert, M., & Lizotte, M. P. (1999). Phytoplankton community structure and the drawdown of nutrients and CO_2 in the Southern Ocean. *Science*, *283*(5400), 365–367. https://doi.org/10.1126/science.283.5400.365

Buchwald, C., & Casciotti, K. L. (2010). Oxygen isotopic fractionation and exchange during bacterial nitrite oxidation. *Limnology & Oceanography*, *55*(3), 1064–1074. https://doi.org/10.4319/lo.2010.55.3.1064

Buchwald, C., & Casciotti, K. L. (2013). Isotopic ratios of nitrite as tracers of the sources and age of oceanic nitrite. *Nature Geoscience*, *6*(4), 308–313. https://doi.org/10.1038/NGEO1745

Buchwald, C., Santoro, A. E., McIlvin, M. R., & Casciotti, K. L. (2012). Oxygen isotopic composition of nitrate and nitrite produced by nitrifying cocultures and natural marine assemblages. *Limnology & Oceanography*, *57*(5), 1361–1375. https://doi.org/10.4319/lo.2012.57.5.1361

Buchwald, C., Santoro, A. E., Stanley, R. H. R., & Casciotti, K. L. (2015). Nitrogen cycling in the secondary nitrite maximum of the eastern tropical North Pacific off Costa Rica. *Global Biogeochemical Cycles*, *29*(12), 2061–2081. https://doi.org/10.1002/2015GB005187

Carvalho, F., Kohut, J., Oliver, M. J., Sherrell, M. J., & Schofield, O. (2016). Mixing and phytoplankton dynamics in a submarine canyon in the West Antarctic Peninsula. *Journal of Geophysical Research: Oceans*, *121*(7), 5069–5083. https://doi.org/10.1002/2016JC011650

Casciotti, K. L. (2009). Inverse kinetic isotope fractionation during bacterial nitrite oxidation. *Geochimica et Cosmochimica Acta*, *73*(7), 2061–2076. https://doi.org/10.1016/j.gca.2008.12.022

Casciotti, K. L. (2016a). Nitrite isotopes as tracers of marine N cycle processes. *Philosophical Transactions of the Royal Society A: Mathematical, Physical & Engineering Sciences*, *374*(2081), 20150295. https://doi.org/10.1098/rsta.2015.0295

Casciotti, K. L. (2016b). Nitrogen and oxygen isotopic studies of the marine nitrogen cycle. *Annual Review of Marine Science*, *8*(1), 379–407. https://doi.org/10.1146/annurev-marine-010213-135052

Casciotti, K. L., Bohlke, J. K., McIlvin, M. R., Mroczkowski, S. J., & Hannon, J. E. (2007). Oxygen isotopes in nitrite: Analysis, calibration, and equilibration. *Analytical Chemistry*, *79*(6), 2427–2436. https://doi.org/10.1021/ac061598h

Casciotti, K. L., Forbes, M., Vedamati, J., Peters, B. D., Martin, T. S., & Mordy, C. W. (2018). Nitrous oxide cycling in the Eastern Tropical South Pacific as inferred from isotopic and isotopomeric data. *Deep-Sea Research Part II Topical Studies in Oceanography*, *156*, 155–167. https://doi.org/10.1016/j.dsr2.2018.07.014

Casciotti, K. L., McIlvin, M., & Buchwald, C. (2010). Oxygen isotopic exchange and fractionation during bacterial ammonia oxidation. *Limnology & Oceanography*, *55*(2), 753–762. https://doi.org/10.4319/lo.2010.55.2.0753

Casciotti, K. L., & McIlvin, M. R. (2007). Isotopic analyses of nitrate and nitrite from reference mixtures and application to Eastern Tropical North Pacific waters. *Marine Chemistry*, *107*(2), 184–201. https://doi.org/10.1016/j.marchem.2007.06.021

Casciotti, K. L., Sigman, D. M., Hastings, M. G., Bohlke, J. K., & Hilkert, A. (2002). Measurement of the oxygen isotopic composition of nitrate in seawater and freshwater using the denitrifier method. *Analytical Chemistry*, *74*(19), 4905–4912. https://doi.org/10.1021/ac020113w

Chen, Y. (2021). *Nitrogen and oxygen isotopes in tracing nitrite cycle in marginal seas* PhD thesis (pp. 1–160). Xiamen University.

Chen, Y., Chen, J., Wang, Y., Jiang, Y., Zheng, M., Qiu, Y., & Chen, M. (2023). Sources and transformations of nitrite in the Amundsen Sea in summer 2019 and 2020 as revealed by nitrogen and oxygen isotopes. *Acta Oceanologica Sinica*, *42*(4), 16–24. https://doi.org/10.1007/s13131-022-2111-4

Chen, Y., Chen, M., Chen, J., Fan, L., Zheng, M., & Qiu, Y. (2022). Dual isotopes of nitrite in the Amundsen Sea in summer. *Science of the Total Environment*, *843*, 157055. https://doi.org/10.1016/j.scitotenv.2022.157055

Chen, Y. J., & Chen, M. (2022). Nitrite cycling in warming Arctic and subarctic waters. *Geophysical Research Letters*, *49*(12), e2021GL096947. https://doi.org/10.1029/2021GL096947

Comiso, J. C., McClain, C. R., Sullivan, C. W., Ryan, J. P., & Leonard, C. L. (1993). Coastal zone color scanner pigment concentrations in the Southern Ocean and relationships to geophysical surface features. *Journal of Geophysical Research*, *98*(C2), 2419–2451. https://doi.org/10.1029/92JC02505

Daims, H., Lücker, S., & Wagner, M. (2016). A new perspective on microbes formerly known as nitrite-oxidizing bacteria. *Trends in Microbiology*, *24*(9), 699–712. https://doi.org/10.1016/j.tim.2016.05.004

DeVries, T. (2014). The oceanic anthropogenic CO_2 sink: Storage, air-sea fluxes, and transports over the industrial era. *Global Biogeochemical Cycles*, *28*(7), 631–647. https://doi.org/10.1002/2013GB004739

DiFiore, P. J., Sigman, D. M., & Dunbar, R. B. (2009). Upper ocean nitrogen fluxes in the Polar Antarctic Zone: Constraints from the nitrogen and oxygen isotopes of nitrate. *Geochemistry, Geophysics, Geosystems*, *10*(11), Q11016. https://doi.org/10.1029/2009GC002468

DiFiore, P. J., Sigman, D. M., Karsh, K. L., Trull, T. W., Dunbar, R. B., & Robinson, R. S. (2010). Poleward decrease in the isotope effect of nitrate assimilation across the Southern Ocean. *Geophysical Research Letters*, *37*(17), L17601. https://doi.org/10.1029/2010GL044090

DiFiore, P. J., Sigman, D. M., Trull, T. W., Lourey, M. J., Karsh, K., Cane, G., & Ho, R. (2006). Nitrogen isotope constraints on subantarctic biogeochemistry. *Journal of Geophysical Research*, *111*(C8), C08016. https://doi.org/10.1029/2005JC003216

Friedman, S. H., Massefski, W., & Hollocher, T. C. (1986). Catalysis of intermolecular oxygen atom transfer by nitrite dehydrogenase of *Nitrobacter agilis*. *Journal of Biological Chemistry*, *261*(23), 10538–10543. https://doi.org/10.1016/S0021-9258(18)67418-6

Fripiat, F., Martinez-Garcia, A., Fawcett, S. E., Kemeny, P. C., Studer, A. S., Smart, S. M., et al. (2019). The isotope effect of nitrate assimilation in the Antarctic Zone: Improved estimates and paleoceanographic implications. *Geochimica et Cosmochimica Acta*, *247*, 261–279. https://doi.org/10.1016/j.gca.2018.12.003

Fripiat, F., Sigman, D. M., Fawcett, S. E., Rafter, P. A., Weigand, M. A., & Tison, J. L. (2014). New insights into sea ice nitrogen biogeochemical dynamics from the nitrogen isotopes. *Global Biogeochemical Cycles*, *28*(2), 115–130. https://doi.org/10.1002/2013GB004729

Gomi, Y., Fukuchi, M., & Taniguchi, A. (2010). Diatom assemblages at subsurface chlorophyll maximum layer in the eastern Indian sector of the Southern Ocean in summer. *Journal of Plankton Research*, *32*(7), 1039–1050. https://doi.org/10.1093/plankt/fbq031

Granger, J., & Sigman, D. M. (2009). Removal of nitrite with sulfamic acid for nitrate N and O isotope analysis with the denitrifier method. *Rapid Communications in Mass Spectrometry*, *23*, 3753–3762. https://doi.org/10.1002/rcm.4307

Granger, J., Sigman, D. M., Needoba, J. A., & Harrison, P. J. (2004). Coupled nitrogen and oxygen isotope fractionation of nitrate during assimilation by cultures of marine phytoplankton. *Limnology & Oceanography*, *49*(5), 1763–1773. https://doi.org/10.4319/lo.2004.49.5.1763

Granger, J., Sigman, D. M., Rohde, M. M., Maldonado, M. T., & Tortell, P. D. (2010). N and O isotope effects during nitrate assimilation by unicellular prokaryotic and eukaryotic plankton cultures. *Geochimica et Cosmochimica Acta*, *74*(3), 1030–1040. https://doi.org/10.1016/j.gca.2009.10.044

Gray, A. R., Johnson, K. S., Bushinsky, S. M., Riser, S. C., Russell, J. L., Talley, L. D., et al. (2018). Autonomous biogeochemical floats detect significant carbon dioxide outgassing in the high-latitude Southern Ocean. *Geophysical Research Letters*, *45*(17), 9049–9057. https://doi.org/10.1029/2018GL078013

Gruber, N., Bakker, D. C., DeVries, T., Gregor, L., Hauck, J., Landschützer, P., et al. (2023). Trends and variability in the ocean carbon sink. *Nature Reviews Earth and Environment*, *4*(2), 119–134. https://doi.org/10.1038/s43017-022-00381-x

Henley, S. F., Jones, E. M., Venables, H. J., Meredith, M. P., Firing, Y. L., Dittrich, R., et al. (2018). Macronutrient and carbon supply, uptake and cycling across the Antarctic Peninsula shelf during summer. *Philosophical Transactions of the Royal Society A: Mathematical, Physical and Engineering Sciences*, *376*(2122), 20170168. https://doi.org/10.1098/rsta.2017.0168

Henley, S. F., Tuerena, R. E., Annett, A. L., Fallick, A. E., Meredith, M. P., Venables, H. J., et al. (2017). Macronutrient supply, uptake and recycling in the coastal ocean of the west Antarctic Peninsula. *Deep-Sea Research Part II Topical Studies in Oceanography*, *139*, 58–76. https://doi.org/10.1016/j.dsr2.2016.10.003

Hoch, M. P., Fogel, M. L., & Kirchman, D. L. (1992). Isotope fractionation associated with ammonium uptake by a marine bacterium. *Limnology & Oceanography*, *37*(7), 1447–1459. https://doi.org/10.4319/lo.1992.37.7.1447

Horn, M. G., Robinson, R. S., Rynearson, T. A., & Sigman, D. M. (2011). Nitrogen isotopic relationship between diatom-bound and bulk organic matter of cultured polar diatoms. *Paleoceanography*, *26*(3). https://doi.org/10.1029/2010PA002080

Huang, W. H., Yang, X. F., Zhao, J., Li, D., & Pan, J. M. (2022). Dissolved nutrient distributions in the Antarctic Cosmonaut Sea in austral summer. *Advances in Polar Science*, *33*, 267–290. https://doi.org/10.13679/j.advps.2022.0099

Hunt, B. P., & Hosie, G. W. (2006). The seasonal succession of zooplankton in the Southern Ocean south of Australia, part I: The seasonal ice zone. *Deep - Sea Research Part I: Oceanographic Research Papers*, *53*(7), 1182–1202. https://doi.org/10.1016/j.dsr.2006.05.001

Hunt, B. P. V., Pakhomov, E. A., & Trotsenko, B. G. (2007). The macrozooplankton of the Cosmonaut Sea, east Antarctica (30°E–60°E), 1987–1990. *Deep - Sea Research Part I: Oceanographic Research Papers*, *54*(7), 1042–1069. https://doi.org/10.1016/j.dsr.2007.04.002

Jang, Y. H., Khim, B. K., Shin, H. C., Sigman, D. M., Wang, Y., & Hong, C. S. (2008). Variation of nitrate concentrations and $\delta^{15}N$ values of seawater in the Drake Passage, Antarctic Ocean. *Ocean and Polar Research*, *30*(4), 407–418. https://doi.org/10.4217/OPR.2008.30.4.407

Karsh, K. L., Granger, J., Kritee, K., & Sigman, D. M. (2012). Eukaryotic assimilatory nitrate reductase fractionates N and O isotopes with a ratio near unity. *Environmental Science and Technology*, *46*(11), 5727–5735. https://doi.org/10.1021/es204593q

Karsh, K. L., Trull, T. W., Lourey, A. J., & Sigman, D. M. (2003). Relationship of nitrogen isotope fractionation to phytoplankton size and iron availability during the Southern Ocean Iron RElease Experiment (SOIREE). *Limnology & Oceanography*, *48*(3), 1058–1068. https://doi.org/10.4319/lo.2003.48.3.1058

Kemeny, P. C., Weigand, M. A., Zhang, R., Carter, B. R., Karsh, K. L., Fawcett, S. E., & Sigman, D. M. (2016). Enzyme-level interconversion of nitrate and nitrite in the fall mixed layer of the Antarctic Ocean. *Global Biogeochemical Cycles*, *30*(7), 1069–1085. https://doi.org/10.1002/2015GB005350

Koch, H., Lücker, S., Albertsen, M., Kitzinger, K., Herbold, C., Spieck, E., et al. (2015). Expanded metabolic versatility of ubiquitous nitrite-oxidizing bacteria from the genus Nitrospira. *Proceedings of the National Academy of Sciences of the United States of America*, *112*(36), 11371–11376. https://doi.org/10.1073/pnas.1506533112

Lannuzel, D., Schoemann, V., De Jong, J., Pasquer, B., van der Merwe, P., Masson, F., et al. (2010). Distribution of dissolved iron in Antarctic sea ice: Spatial, seasonal, and inter-annual variability. *Journal of Geophysical Research*, *115*(G3). https://doi.org/10.1029/2009JG001031

Lehmann, M. F., Bernasconi, S. M., Barbieri, A., & McKenzie, J. A. (2002). Preservation of organic matter and alteration of its carbon and nitrogen isotope composition during simulated and in situ early sedimentary diagenesis. *Geochimica et Cosmochimica Acta*, *66*(20), 3573–3584. https://doi.org/10.1016/S0016-7037(02)00968-7

Li, Z., Xu, C., Zheng, M., Chen, M., Qiu, Y., Zhou, H., et al. (2023). Nitrate isotope dynamics in the lower euphotic-upper mesopelagic zones of the western South China Sea. *Acta Oceanologica Sinica*, *42*, 1–11. https://doi.org/10.1007/s13131-022-2091-4

Liu, K. K., Kao, S. J., Chiang, K. P., Gong, G. C., Chang, J., Cheng, J. S., & Lan, C. Y. (2013). Concentration dependent nitrogen isotope fractionation during ammonium uptake by phytoplankton under an algal bloom condition in the Danshuei estuary, northern Taiwan. *Marine Chemistry*, *157*, 242–252. https://doi.org/10.1016/j.marchem.2013.10.005

Liu, S. M., Ning, X., Dong, S., Song, G., Wang, L., Altabet, M. A., et al. (2020). Source versus recycling influences on the isotopic composition of nitrate and nitrite in the East China Sea. *Journal of Geophysical Research: Oceans*, *125*(8), e2020JC016061. https://doi.org/10.1029/2020JC016061

Mariotti, A., Germon, J., Hubert, P., Kaiser, P., Letolle, R., Tardieux, A., & Tardieux, P. (1981). Experimental determination of nitrogen kinetic isotope fractionation: Some principles; illustration for the denitrification and nitrification processes. *Plant and Soil*, *62*(3), 413–430. https://doi.org/10.1007/bf02374138

McIlvin, M. R., & Altabet, M. A. (2005). Chemical conversion of nitrate and nitrite to nitrous oxide for nitrogen and oxygen isotopic analysis in freshwater and seawater. *Analytical Chemistry*, *77*(17), 5589–5595. https://doi.org/10.1021/ac050528s

Mitchell, B. G., Brody, E. A., Holm-Hansen, O., McClain, C., & Bishop, J. (1991). Light limitation of phytoplankton biomass and macronutrient utilization in the Southern Ocean. *Limnology & Oceanography*, *36*(8), 1662–1677. https://doi.org/10.4319/lo.1991.36.8.1662

Montoya, J. P., & McCarthy, J. J. (1995). Isotopic fractionation during nitrate uptake by phytoplankton grown in continuous culture. *Journal of Plankton Research*, *17*(3), 439–464. https://doi.org/10.1093/plankt/17.3.439

Mooshammer, M., Alves, R. J. E., Bayer, B., Melcher, M., Stieglmeier, M., Jochum, L., et al. (2020). Nitrogen isotope fractionation during archaeal ammonia oxidation: Coupled estimates from measurements of residual ammonium and accumulated nitrite. *Frontiers in Microbiology*, *11*, 1710. https://doi.org/10.3389/fmicb.2020.01710

Needoba, J. A., & Harrison, P. J. (2004). Influence of low light and a light/dark cycle on NO_3^- uptake, intracellular NO_3^-, and nitrogen isotope fractionation by marine phytoplankton. *Journal of Phycology*, *40*(3), 505–516. https://doi.org/10.1111/j.1529-8817.2004.03171.x

Nicol, S., Pauly, T., Bindoff, N. L., Wright, S., Thiele, D., Hosie, G. W., et al. (2000). Ocean circulation off east Antarctica affects ecosystem structure and sea-ice extent. *Nature*, *406*(6795), 504–507. https://doi.org/10.1038/35020053

Nishizawa, M., Sakai, S., Konno, U., Nakahara, N., Takaki, Y., Saito, Y., et al. (2016). Nitrogen and oxygen isotope effects of ammonia oxidation by *thermophilic Thaumarchaeota* from a geothermal water stream. *Applied and Environmental Microbiology*, *82*(15), 4492–4504. https://doi.org/10.1128/AEM.00250-16

Nissen, C., Gruber, N., Münnich, M., & Vogt, M. (2021). Southern Ocean phytoplankton community structure as a gatekeeper for global nutrient biogeochemistry. *Global Biogeochemical Cycles*, *35*(8), e2021GB006991. https://doi.org/10.1029/2021GB006991

Orsi, A. H., Whitworth, T., & Nowlin, W. D. (1995). On the meridional extent and fronts of the Antarctic Circumpolar Current. *Deep - Sea Research Part I: Oceanographic Research Papers*, *42*(5), 641–673. https://doi.org/10.1016/0967-0637(95)00021-W

Qi, Q., Hao, Q., Yang, G., Cao, S., Kang, J., Hu, J., et al. (2024). Diverse impacts of sea ice and ice shelf melting on phytoplankton communities in the Cosmonaut Sea, East Antarctica. *Environmental Research Letters*, *20*(1), 014003. https://doi.org/10.1088/1748-9326/ad975e

Rafter, P. A., DiFiore, P. J., & Sigman, D. M. (2013). Coupled nitrate nitrogen and oxygen isotopes and organic matter remineralization in the Southern and Pacific Oceans. *Journal of Geophysical Research: Oceans*, *118*(10), 4781–4794. https://doi.org/10.1002/jgrc.20316

Santoro, A. E., & Casciotti, K. L. (2011). Enrichment and characterization of ammonia-oxidizing archaea from the open ocean: Phylogeny, physiology and stable isotope fractionation. *The ISME Journal*, *5*(11), 1796–1808. https://doi.org/10.1038/ismej.2011.58

Sarmiento, J. L., Gruber, N., Brzezinski, M. A., & Dunne, J. P. (2004). High-latitude controls of thermocline nutrients and low latitude biological productivity. *Nature*, *427*(6969), 56–60. https://doi.org/10.1038/nature02127

Sarmiento, J. L., & Toggweiler, J. (1984). A new model for the role of the oceans in determining atmospheric pCO_2. *Nature*, *308*(5960), 621–624. https://doi.org/10.1038/308621a0

Sedwick, P. N., DiTullio, G. R., & Mackey, D. J. (2000). Iron and manganese in the Ross Sea, Antarctica: Seasonal iron limitation in Antarctic shelf waters. *Journal of Geophysical Research*, *105*(C5), 11321–11336. https://doi.org/10.1029/2000JC000256

Siegenthaler, U., & Wenk, T. (1984). Rapid atmospheric CO_2 variations and ocean circulation. *Nature*, *308*(5960), 624–626. https://doi.org/10.1038/308624a0

Sigman, D. M., Altabet, M. A., McCorkle, D. C., Francois, R., & Fischer, G. (1999). The $\delta^{15}N$ of nitrate in the Southern Ocean: Consumption of nitrate in surface waters. *Global Biogeochemical Cycles*, *13*(4), 1149–1166. https://doi.org/10.1029/1999GB900038

Sigman, D. M., Altabet, M. A., McCorkle, D. C., Francois, R., & Fischer, G. (2000). The $\delta^{15}N$ of nitrate in the Southern Ocean: Nitrogen cycling and circulation in the ocean interior. *Journal of Geophysical Research*, *105*(C8), 19599–19614. https://doi.org/10.1029/2000JC000265

Sigman, D. M., Casciotti, K. L., Andreani, M., Barford, C., Galanter, M., & Bohlke, J. K. (2001). A bacterial method for the nitrogen isotopic analysis of nitrate in seawater and freshwater. *Analytical Chemistry*, *73*(17), 4145–4153. https://doi.org/10.1021/ac010088e

Sigman, D. M., Hain, M. P., & Haug, G. H. (2010). The polar ocean and glacial cycles in atmospheric CO_2 concentration. *Nature*, *466*(7302), 47–55. https://doi.org/10.1038/nature09149

Smart, S. M., Fawcett, S. E., Thomalla, S. J., Weigand, M. A., Reason, C. J. C., & Sigman, D. M. (2015). Isotopic evidence for nitrification in the Antarctic winter mixed layer. *Global Biogeochemical Cycles*, *29*(4), 427–445. https://doi.org/10.1002/2014GB005013

Smith, A. J. R., Ratnarajah, L., Holmes, T. M., Wuttig, K., Townsend, A. T., Westwood, K., et al. (2021). Circumpolar deep water and shelf sediments support late summer microbial iron remineralization. *Global Biogeochemical Cycles*, *35*(11), e2020GB006921. https://doi.org/10.1029/2020GB006921

Sundermeyer-Klinger, H., Meyer, W., Warninghoff, B., & Bock, E. (1984). Membrane-bound nitrite oxidoreductase of Nitrobacter: Evidence for a nitrate reductase system. *Archives of Microbiology*, *140*(2–3), 153–158. https://doi.org/10.1007/BF00454918

Tagliabue, A., Bopp, L., & Aumont, O. (2009). Evaluating the importance of atmospheric and sedimentary iron sources to Southern Ocean biogeochemistry. *Geophysical Research Letters*, *36*(13), L13601. https://doi.org/10.1029/2009GL038914

Tagliabue, A., Sallée, J. B., Bowie, A. R., Lévy, M., Swart, S., & Boyd, P. W. (2014). Surface-water iron supplies in the Southern Ocean sustained by deep winter mixing. *Nature Geoscience*, *7*, 314–320. https://doi.org/10.1038/NGE02101

Takeda, S. (1998). Influence of iron availability on nutrient consumption ratio of diatoms in oceanic waters. *Nature*, *393*(6687), 774–777. https://doi.org/10.1038/31674

Tamura, T. P., Nomura, D., Hirano, D., Tamura, T., Kiuchi, M., Hashida, G., et al. (2023). Impacts of basal melting of the Totten Ice Shelf and biological productivity on marine biogeochemical components in Sabrina Coast, East Antarctica. *Global Biogeochemical Cycles*, *37*(9), e2022GB007510. https://doi.org/10.1029/2022GB007510

Tynan, C. T. (1998). Ecological importance of the southern boundary of the Antarctic circumpolar current. *Nature*, *392*(6677), 708–710. https://doi.org/10.1038/33675

Waser, N. A. D., Harrison, P. J., Nielsen, B., Calvert, S. E., & Turpin, D. H. (1998). Nitrogen isotope fractionation during the uptake and assimilation of nitrate, nitrite, ammonium, and urea by a marine diatom. *Limnology & Oceanography*, *43*(2), 215–224. https://doi.org/10.4319/lo.1998.43.2.0215

Weigand, M. A., Foriel, J., Barnett, B., Oleynik, S., & Sigman, D. M. (2016). Updates to instrumentation and protocols for isotopic analysis of nitrate by the denitrifier method. *Rapid Communications in Mass Spectrometry*, *30*(12), 1365–1383. https://doi.org/10.1002/rcm.7570

Williams, G. D., Nicol, S., Aoki, S., Meijers, A. J. S., Bindoff, N. L., Iijima, Y., et al. (2010). Surface oceanography of BROKE-West, along the Antarctic margin of the south-west Indian Ocean (30–80°E). *Deep-Sea Research Part II Topical Studies in Oceanography*, *57*(9–10), 738–757. https://doi.org/10.1016/j.dsr2.2009.04.020

Wright, S. W., & van den Enden, R. L. (2000). Phytoplankton community structure and stocks in the East Antarctic marginal ice zone (BROKE survey, January–March 1996) determined by CHEMTAX analysis of HPLC pigment signatures. *Deep-Sea Research Part II Topical Studies in Oceanography*, *47*(12–13), 2363–2400. https://doi.org/10.1016/S0967-0645(00)00029-1

Wulff, A., & Wängberg, S. Å. (2004). Spatial and vertical distribution of phytoplankton pigments in the eastern Atlantic sector of the Southern Ocean. *Deep-Sea Research Part II Topical Studies in Oceanography*, *51*(22–24), 2701–2713. https://doi.org/10.1016/j.dsr2.2001.01.002

Wunderlich, A., Meckenstock, R. U., & Einsiedl, F. (2013). A mixture of nitrite-oxidizing and denitrifying microorganisms affects the $\delta^{18}O$ of dissolved nitrate during anaerobic microbial denitrification depending on the $\delta^{18}O$ of ambient water. *Geochimica et Cosmochimica Acta*, *119*, 31–45. https://doi.org/10.1016/j.gca.2013.05.028

Yamazaki, K., Aoki, S., Katsumata, K., Hirano, D., & Nakayama, Y. (2021). Multidecadal poleward shift of the southern boundary of the Antarctic circumpolar current off East Antarctica. *Science Advances*, *7*(24), eabf8755. https://doi.org/10.1126/sciadv.abf8755

Yang, G., Mou, W., Chen, X., Xu, Z., Wang, Y., & Li, C. (2022). Vertical occurrence of copepod carcasses in the Cosmonaut Sea during austral summer. *Deep - Sea Research Part II: Topical Studies in Oceanography*, *198*, 105051. https://doi.org/10.1016/j.dsr2.2022.105051

Zu, Y. C., Gao, L. B., Guo, G. J., & Fang, Y. (2022). Changes of circumpolar deep water between 2006 and 2020 in the south-west Indian Ocean, East Antarctica. *Deep-Sea Research Part II Topical Studies in Oceanography*, *197*, 105043. https://doi.org/10.1016/j.dsr2.2022.105043